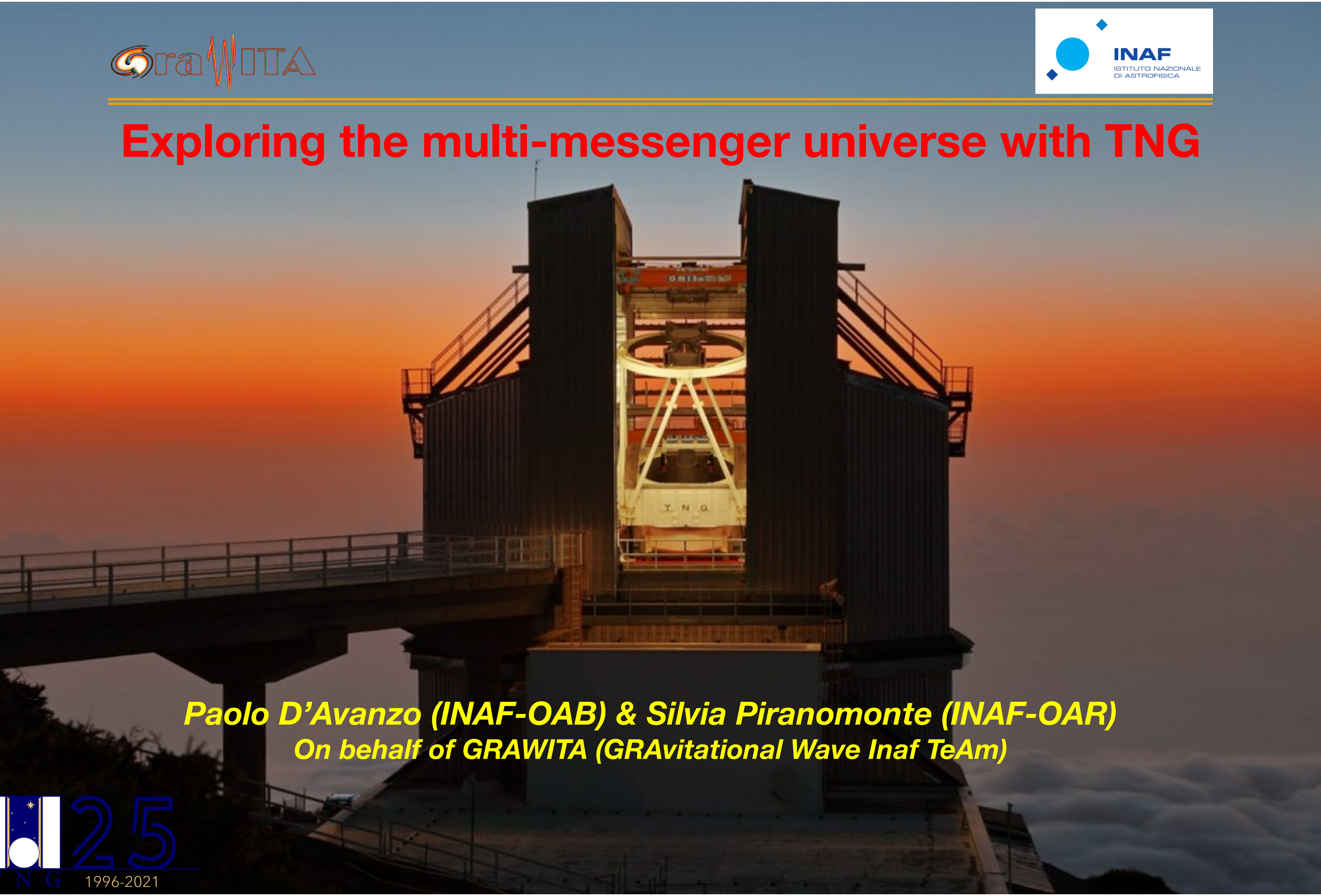

Exploring the multi-messenger universe with TNG

Paolo D’Avanzo (INAF-OAB) & Silvia Piranomonte (INAF-OAR)
On behalf of GRAWITA (GRAvitational Wave Inaf TeAm)

1996-2021

The Multi-Messenger era

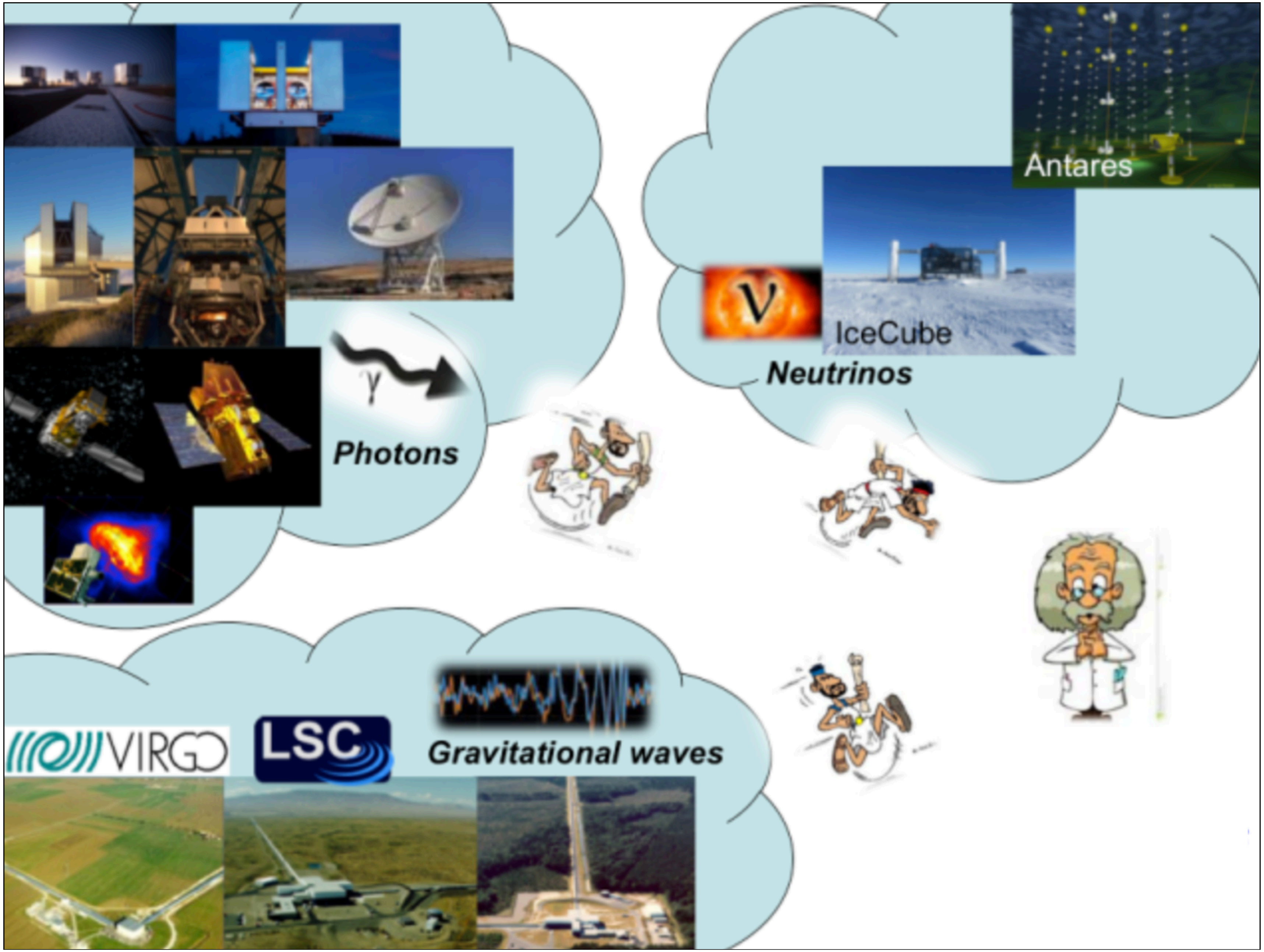

The GW era

LIGO Hanford
GEO 600
Virgo
KAGRA
LIGO Livingston
LIGO-India

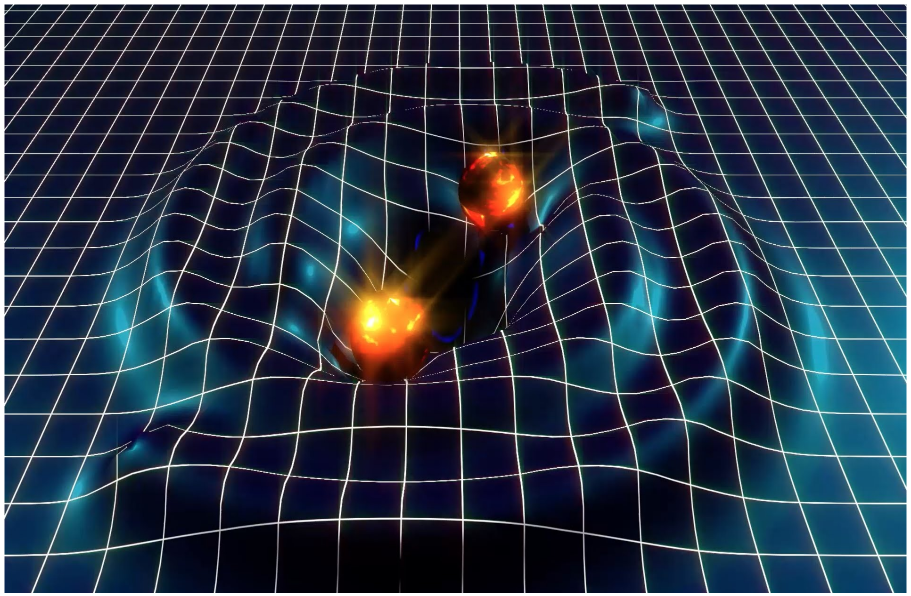

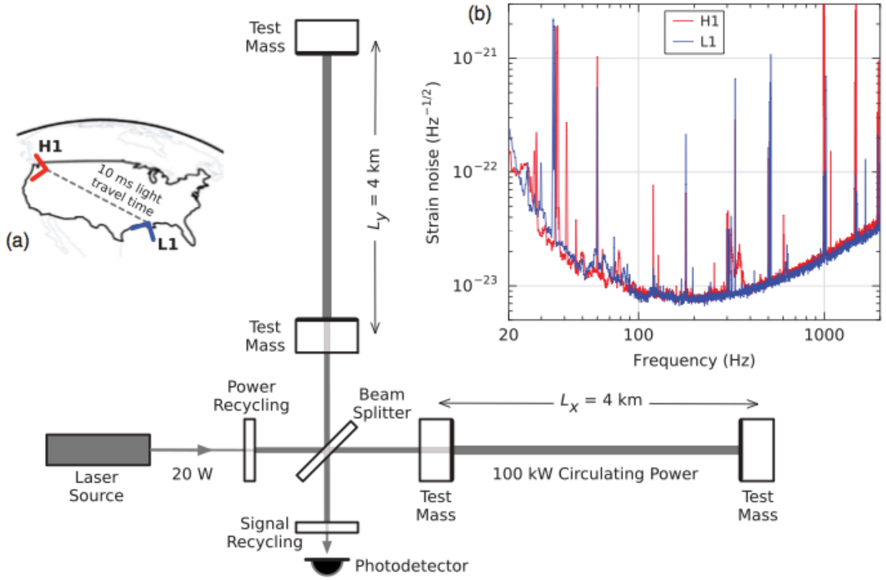

H1
10 ms light travel time
L1
(a)
Test Mass
Test Mass
L_y = 4 km
Power Recycling
Beam Splitter
L_x = 4 km
Laser Source
20 W
100 kW Circulating Power
Test Mass
Test Mass
Signal Recycling
Photodetector
(b)
H1
L1
Strain noise (Hz$^{-1/2}$)
10^{-21}
10^{-22}
10^{-23}
20
100
1000
Frequency (Hz)

The GW era: GW 150914

Selected for a Viewpoint in *Physics*
PRL **116,** 061102 (2016) PHYSICAL REVIEW LETTERS week ending 12 FEBRUARY 2016

Observation of Gravitational Waves from a Binary Black Hole Merger

B. P. Abbott *et al.**
(LIGO Scientific Collaboration and Virgo Collaboration)
(Received 21 January 2016; published 11 February 2016)

On September 14, 2015 at 09:50:45 UTC the two detectors of the Laser Interferometer Gravitational-Wave Observatory simultaneously observed a transient gravitational-wave signal. The signal sweeps upwards in frequency from 35 to 250 Hz with a peak gravitational-wave strain of 1.0×10^{-21}. It matches the waveform predicted by general relativity for the inspiral and merger of a pair of black holes and the ringdown of the resulting single black hole. The signal was observed with a matched-filter signal-to-noise ratio of 24 and a false alarm rate estimated to be less than 1 event per 203 000 years, equivalent to a significance greater than 5.1σ. The source lies at a luminosity distance of 410^{+160}_{-180} Mpc corresponding to a redshift $z = 0.09^{+0.03}_{-0.04}$. In the source frame, the initial black hole masses are $36^{+5}_{-4} M_\odot$ and $29^{+4}_{-4} M_\odot$, and the final black hole mass is $62^{+4}_{-4} M_\odot$, with $3.0^{+0.5}_{-0.5} M_\odot c^2$ radiated in gravitational waves. All uncertainties define 90% credible intervals. These observations demonstrate the existence of binary stellar-mass black hole systems. This is the first direct detection of gravitational waves and the first observation of a binary black hole merger.

DOI: 10.1103/PhysRevLett.116.061102

Primary black hole mass	$36^{+5}_{-4} M_\odot$
Secondary black hole mass	$29^{+4}_{-4} M_\odot$
Final black hole mass	$62^{+4}_{-4} M_\odot$
Final black hole spin	$0.67^{+0.05}_{-0.07}$
Luminosity distance	410^{+160}_{-180} Mpc
Source redshift z	$0.09^{+0.03}_{-0.04}$

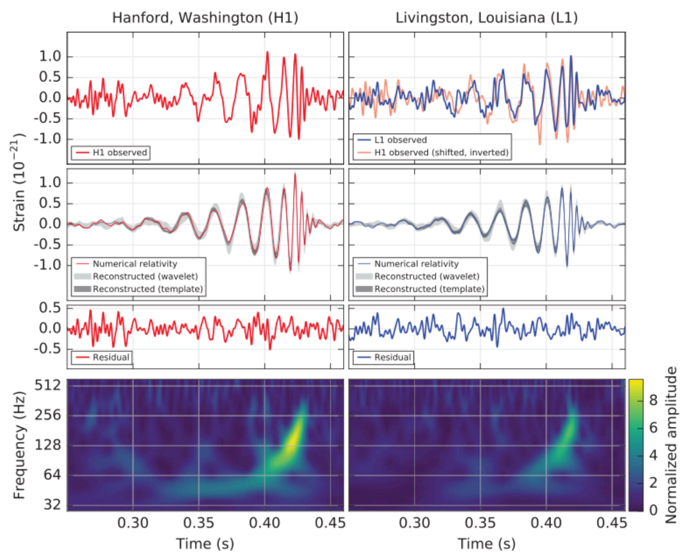

GRAvitational Wave Inaf TeAm

GRAWITA Organization chart

Science Board
E. Brocato (P.I.),
E. Palazzi, E. Cappellaro,
A. Grado, M. Branchesi,
S. Covino, A. Possenti

WG1
24H/7d OPERATION TEAM
P. D'Avanzo

WG2
WIDE FIELD SEARCH
F. Getman

WG3
CHARACTERIZATION and FOLLOW-UP Optical and NIR
A. Melandri

WG4
RADIO Follow-up
M. Orienti

WG5
HIGH ENERGY Prompt and Follow-up
A. Bulgarelli

WG6
THEORETICAL MODELS
R. Ciolfi

WG7
ARCHIVING and WEB ACTIVITIES
L. Nicastro

~ 90 scientists from 21 Institutes (mainly INAF)

Follow-up strategy

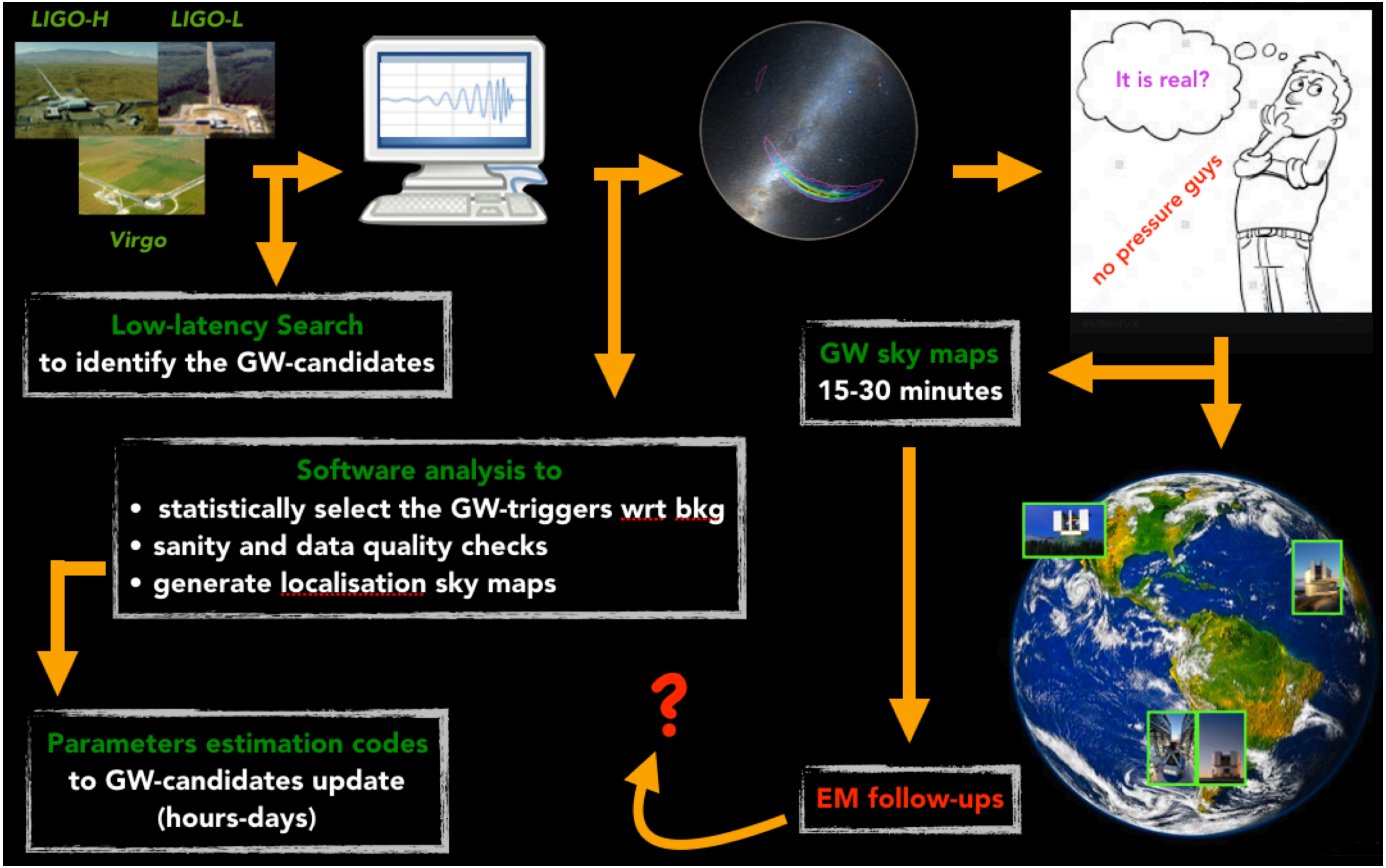

Follow-up strategy

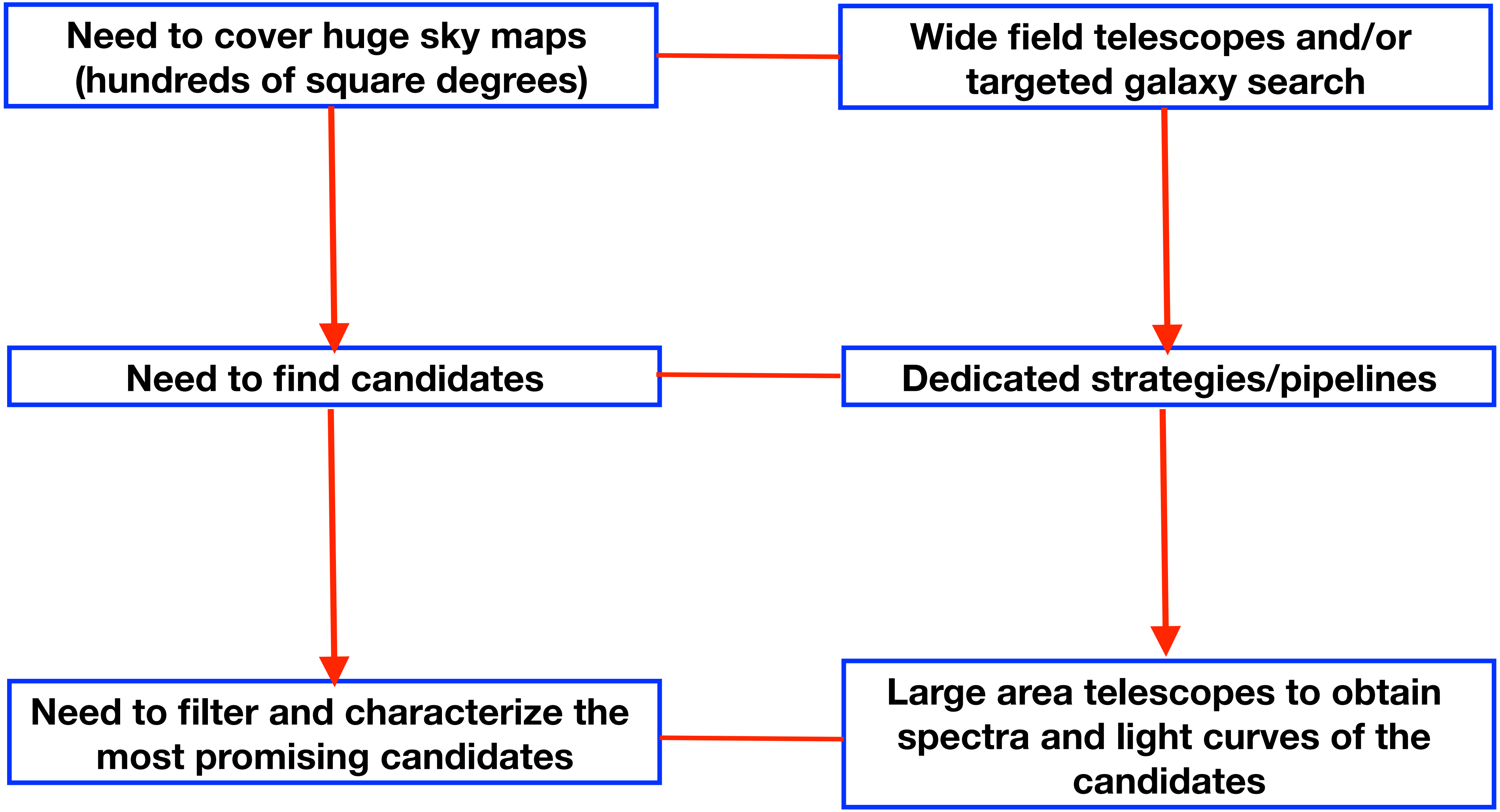

Facilities

+ EVN & e-MERLIN

synergies with high-energy space observatories (Swift, AGILE, INTEGRAL, Fermi)

NS-NS / NS-BH electromagnetic counterparts

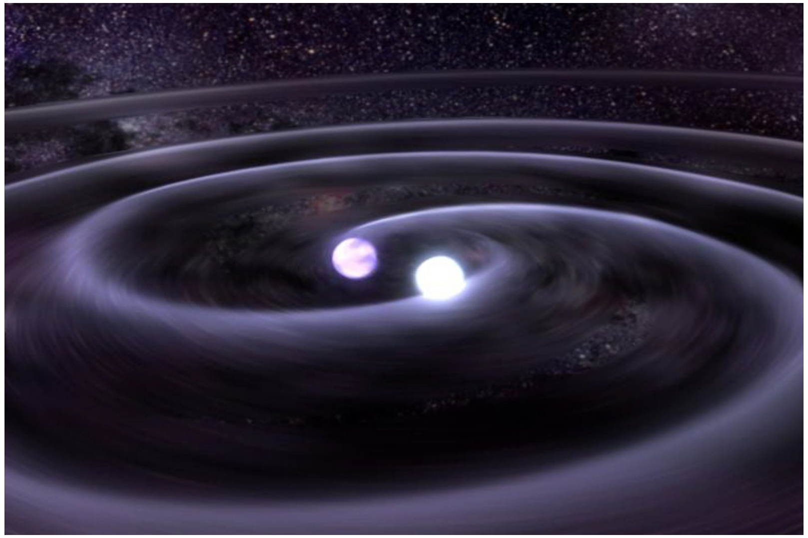

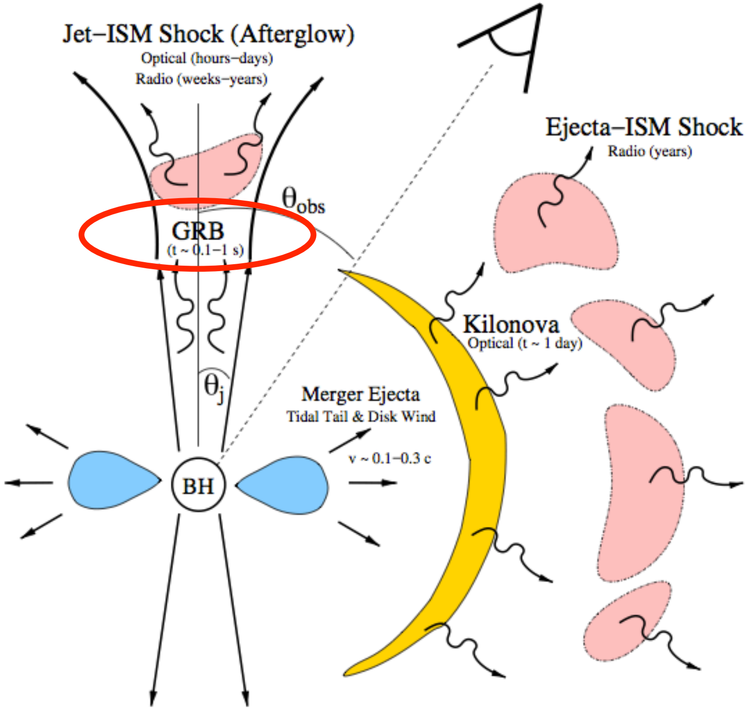

Metzger & Berger 2012

Short GRB

Andrea Melandri's talk

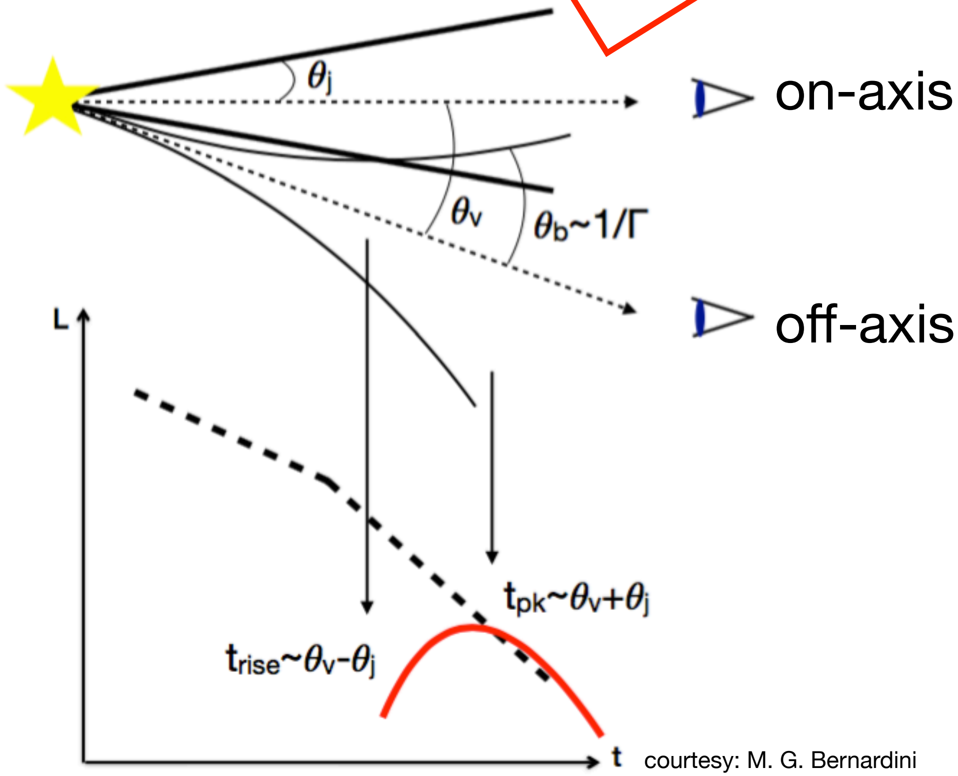

courtesy: M. G. Bernardini

NS-NS / NS-BH electromagnetic counterparts

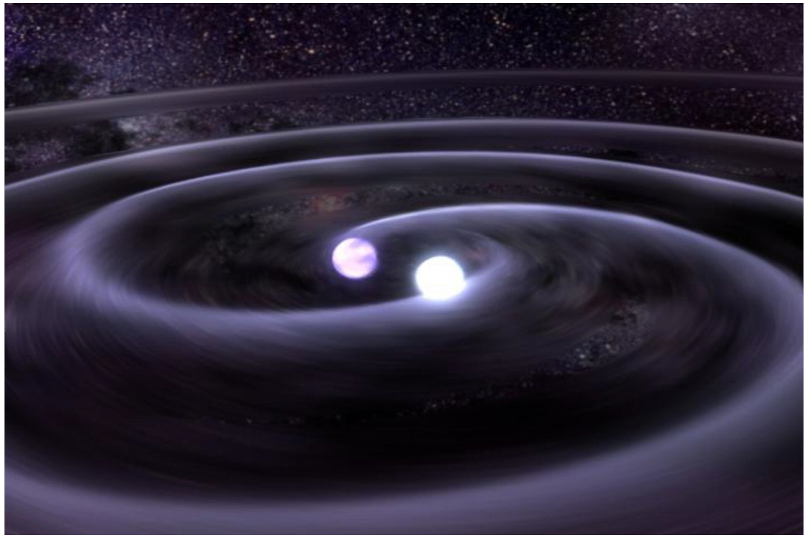

Kilonova (aka macronova)

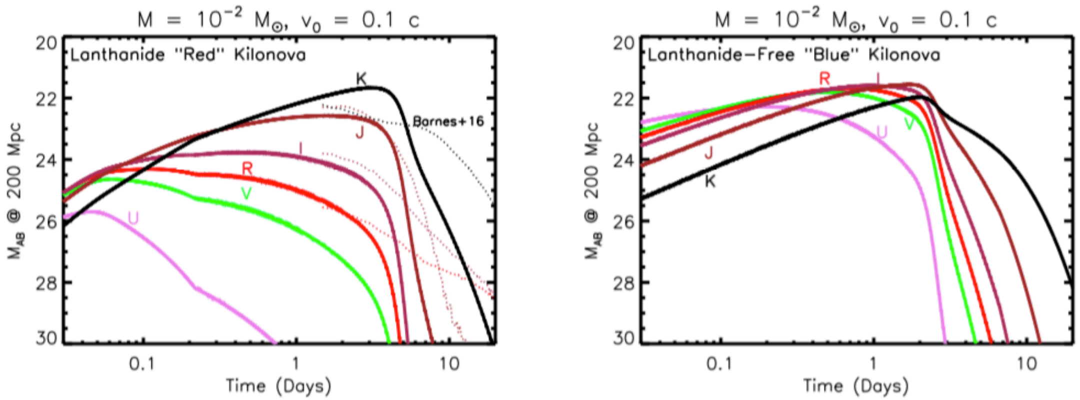

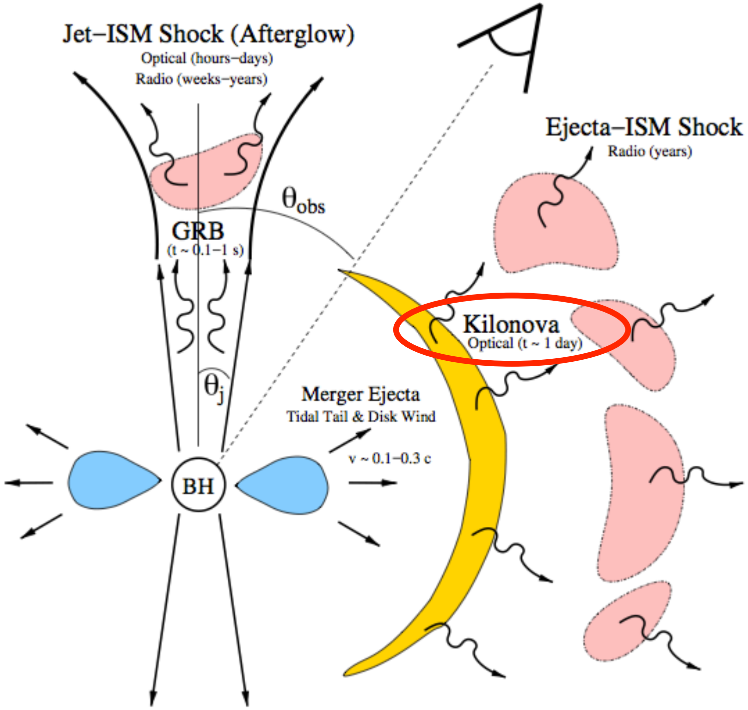

Metzger & Berger 2012

A key signature of an NS–NS/NS–BH binary merger is the production of a so-called "kilonova" (aka "macronova") due to the decay of heavy radioactive species produced by the *r*-process and ejected during the merger that is expected to provide a source of heating and radiation (Li and Paczynski 1998; Rosswog, 2005; Metzger et al., 2010).

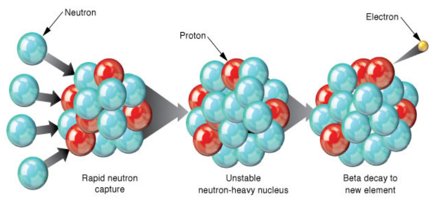

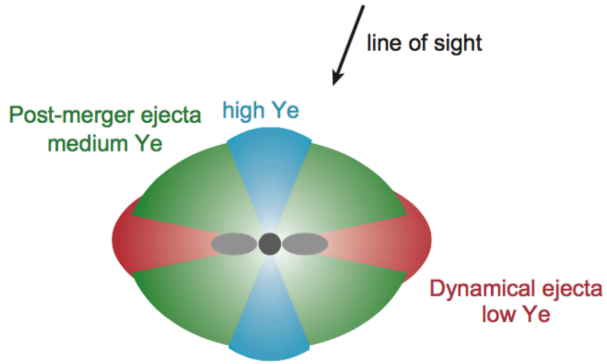

Tanaka et al. (2017)

BH-BH electromagnetic counterparts

BH-BH electromagnetic counterparts

The GW era – O1 & O2

Sept 2015 – Jan 2016: LVC O1 science run
Nov 2016 – Aug 2017: LVC O2 science run

Event	$m_1/\mathrm{M}_\odot$	$m_2/\mathrm{M}_\odot$	$\mathcal{M}/\mathrm{M}_\odot$	χ_{eff}	$M_{\mathrm{f}}/\mathrm{M}_\odot$	a_{f}	$E_{\mathrm{rad}}/(\mathrm{M}_\odot c^2)$	$\ell_{\mathrm{peak}}/(\mathrm{erg\,s^{-1}})$	d_L/Mpc	z	$\Delta\Omega/\mathrm{deg}^2$
GW150914	$35.6^{+4.8}_{-3.0}$	$30.6^{+3.0}_{-4.4}$	$28.6^{+1.6}_{-1.5}$	$-0.01^{+0.12}_{-0.13}$	$63.1^{+3.3}_{-3.0}$	$0.69^{+0.05}_{-0.04}$	$3.1^{+0.4}_{-0.4}$	$3.6^{+0.4}_{-0.4} \times 10^{56}$	430^{+150}_{-170}	$0.09^{+0.03}_{-0.03}$	180
GW151012	$23.3^{+14.0}_{-5.5}$	$13.6^{+4.1}_{-4.8}$	$15.2^{+2.0}_{-1.1}$	$0.04^{+0.28}_{-0.19}$	$35.7^{+9.9}_{-3.8}$	$0.67^{+0.13}_{-0.11}$	$1.5^{+0.5}_{-0.5}$	$3.2^{+0.8}_{-1.7} \times 10^{56}$	1060^{+540}_{-480}	$0.21^{+0.09}_{-0.09}$	1555
GW151226	$13.7^{+8.8}_{-3.2}$	$7.7^{+2.2}_{-2.6}$	$8.9^{+0.3}_{-0.3}$	$0.18^{+0.20}_{-0.12}$	$20.5^{+6.4}_{-1.5}$	$0.74^{+0.07}_{-0.05}$	$1.0^{+0.1}_{-0.2}$	$3.4^{+0.7}_{-1.7} \times 10^{56}$	440^{+180}_{-190}	$0.09^{+0.04}_{-0.04}$	1033
GW170104	$31.0^{+7.2}_{-5.6}$	$20.1^{+4.9}_{-4.5}$	$21.5^{+2.1}_{-1.7}$	$-0.04^{+0.17}_{-0.20}$	$49.1^{+5.2}_{-3.9}$	$0.66^{+0.08}_{-0.10}$	$2.2^{+0.5}_{-0.5}$	$3.3^{+0.6}_{-0.9} \times 10^{56}$	960^{+430}_{-410}	$0.19^{+0.07}_{-0.08}$	924
GW170608	$10.9^{+5.3}_{-1.7}$	$7.6^{+1.3}_{-2.1}$	$7.9^{+0.2}_{-0.2}$	$0.03^{+0.19}_{-0.07}$	$17.8^{+3.2}_{-0.7}$	$0.69^{+0.04}_{-0.04}$	$0.9^{+0.05}_{-0.1}$	$3.5^{+0.4}_{-1.3} \times 10^{56}$	320^{+120}_{-110}	$0.07^{+0.02}_{-0.02}$	396
GW170729	$50.6^{+16.6}_{-10.2}$	$34.3^{+9.1}_{-10.1}$	$35.7^{+6.5}_{-4.7}$	$0.36^{+0.21}_{-0.25}$	$80.3^{+14.6}_{-10.2}$	$0.81^{+0.07}_{-0.13}$	$4.8^{+1.7}_{-1.7}$	$4.2^{+0.9}_{-1.5} \times 10^{56}$	2750^{+1350}_{-1320}	$0.48^{+0.19}_{-0.20}$	1033
GW170809	$35.2^{+8.3}_{-6.0}$	$23.8^{+5.2}_{-5.1}$	$25.0^{+2.1}_{-1.6}$	$0.07^{+0.16}_{-0.16}$	$56.4^{+5.2}_{-3.7}$	$0.70^{+0.08}_{-0.09}$	$2.7^{+0.6}_{-0.6}$	$3.5^{+0.6}_{-0.9} \times 10^{56}$	990^{+320}_{-380}	$0.20^{+0.05}_{-0.07}$	340
GW170814	$30.7^{+5.7}_{-3.0}$	$25.3^{+2.9}_{-4.1}$	$24.2^{+1.4}_{-1.1}$	$0.07^{+0.12}_{-0.11}$	$53.4^{+3.2}_{-2.4}$	$0.72^{+0.07}_{-0.05}$	$2.7^{+0.4}_{-0.3}$	$3.7^{+0.4}_{-0.5} \times 10^{56}$	580^{+160}_{-210}	$0.12^{+0.03}_{-0.04}$	87
GW170817	$1.46^{+0.12}_{-0.10}$	$1.27^{+0.09}_{-0.09}$	$1.186^{+0.001}_{-0.001}$	$0.00^{+0.02}_{-0.01}$	≤ 2.8	≤ 0.89	≥ 0.04	$\geq 0.1 \times 10^{56}$	40^{+10}_{-10}	$0.01^{+0.00}_{-0.00}$	16
GW170818	$35.5^{+7.5}_{-4.7}$	$26.8^{+4.3}_{-5.2}$	$26.7^{+2.1}_{-1.7}$	$-0.09^{+0.18}_{-0.21}$	$59.8^{+4.8}_{-3.8}$	$0.67^{+0.07}_{-0.08}$	$2.7^{+0.5}_{-0.5}$	$3.4^{+0.5}_{-0.7} \times 10^{56}$	1020^{+430}_{-360}	$0.20^{+0.07}_{-0.07}$	39
GW170823	$39.6^{+10.0}_{-6.6}$	$29.4^{+6.3}_{-7.1}$	$29.3^{+4.2}_{-3.2}$	$0.08^{+0.20}_{-0.22}$	$65.6^{+9.4}_{-6.6}$	$0.71^{+0.08}_{-0.10}$	$3.3^{+0.9}_{-0.8}$	$3.6^{+0.6}_{-0.9} \times 10^{56}$	1850^{+840}_{-840}	$0.34^{+0.13}_{-0.14}$	1651

Abbott+19

The GW era – O1 & O2

Sept 2015 – Jan 2016: LVC O1 science run
Nov 2016 – Aug 2017: LVC O2 science run

Event	$m_1/M_\odot$	$m_2/M_\odot$	$\mathcal{M}/M_\odot$	χ_{eff}	$M_f/M_\odot$	a_f	$E_{rad}/(M_\odot c^2)$	$\ell_{peak}/(\mathrm{erg\,s^{-1}})$	d_L/Mpc	z	$\Delta\Omega/\mathrm{deg}^2$
GW150914	$35.6^{+4.8}_{-3.0}$	$30.6^{+3.0}_{-4.4}$	$28.6^{+1.6}_{-1.5}$	$-0.01^{+0.12}_{-0.13}$	$63.1^{+3.3}_{-3.0}$	$0.69^{+0.05}_{-0.04}$	$3.1^{+0.4}_{-0.4}$	$3.6^{+0.4}_{-0.4}\times10^{56}$	430^{+150}_{-170}	$0.09^{+0.03}_{-0.03}$	180
GW151012	$23.3^{+14.0}_{-5.5}$	$13.6^{+4.1}_{-4.8}$	$15.2^{+2.0}_{-1.1}$	$0.04^{+0.28}_{-0.19}$	$35.7^{+9.9}_{-3.8}$	$0.67^{+0.13}_{-0.11}$	$1.5^{+0.5}_{-0.5}$	$3.2^{+0.8}_{-1.7}\times10^{56}$	1060^{+540}_{-480}	$0.21^{+0.09}_{-0.09}$	1555
GW151226	$13.7^{+8.8}_{-3.2}$	$7.7^{+2.2}_{-2.6}$	$8.9^{+0.3}_{-0.3}$	$0.18^{+0.20}_{-0.12}$	$20.5^{+6.4}_{-1.5}$	$0.74^{+0.07}_{-0.05}$	$1.0^{+0.1}_{-0.2}$	$3.4^{+0.7}_{-1.7}\times10^{56}$	440^{+180}_{-190}	$0.09^{+0.04}_{-0.04}$	1033
GW170104	$31.0^{+7.2}_{-5.6}$	$20.1^{+4.9}_{-4.5}$	$21.5^{+2.1}_{-1.7}$	$-0.04^{+0.17}_{-0.20}$	$49.1^{+5.2}_{-3.9}$	$0.66^{+0.08}_{-0.10}$	$2.2^{+0.5}_{-0.5}$	$3.3^{+0.6}_{-0.9}\times10^{56}$	960^{+430}_{-410}	$0.19^{+0.07}_{-0.08}$	924
GW170608	$10.9^{+5.3}_{-1.7}$	$7.6^{+1.3}_{-2.1}$	$7.9^{+0.2}_{-0.2}$	$0.03^{+0.19}_{-0.07}$	$17.8^{+3.2}_{-0.7}$	$0.69^{+0.04}_{-0.04}$	$0.9^{+0.05}_{-0.1}$	$3.5^{+0.4}_{-1.3}\times10^{56}$	320^{+120}_{-110}	$0.07^{+0.02}_{-0.02}$	396
GW170729	$50.6^{+16.6}_{-10.2}$	$34.3^{+9.1}_{-10.1}$	$35.7^{+6.5}_{-4.7}$	$0.36^{+0.21}_{-0.25}$	$80.3^{+14.6}_{-10.2}$	$0.81^{+0.07}_{-0.13}$	$4.8^{+1.7}_{-1.7}$	$4.2^{+0.9}_{-1.5}\times10^{56}$	2750^{+1350}_{-1320}	$0.48^{+0.19}_{-0.20}$	1033
GW170809	$35.2^{+8.3}_{-6.0}$	$23.8^{+5.2}_{-5.1}$	$25.0^{+2.1}_{-1.6}$	$0.07^{+0.16}_{-0.16}$	$56.4^{+5.2}_{-3.7}$	$0.70^{+0.08}_{-0.09}$	$2.7^{+0.6}_{-0.6}$	$3.5^{+0.6}_{-0.9}\times10^{56}$	990^{+320}_{-380}	$0.20^{+0.05}_{-0.07}$	340
GW170814	$30.7^{+5.7}_{-3.0}$	$25.3^{+2.9}_{-4.1}$	$24.2^{+1.4}_{-1.1}$	$0.07^{+0.12}_{-0.11}$	$53.4^{+3.2}_{-2.4}$	$0.72^{+0.07}_{-0.05}$	$2.7^{+0.4}_{-0.3}$	$3.7^{+0.4}_{-0.5}\times10^{56}$	580^{+160}_{-210}	$0.12^{+0.03}_{-0.04}$	87
GW170817	$1.46^{+0.12}_{-0.10}$	$1.27^{+0.09}_{-0.09}$	$1.186^{+0.001}_{-0.001}$	$0.00^{+0.02}_{-0.01}$	≤ 2.8	≤ 0.89	≥ 0.04	$\geq 0.1\times10^{56}$	40^{+10}_{-10}	$0.01^{+0.00}_{-0.00}$	16
GW170818	$35.5^{+7.5}_{-4.7}$	$26.8^{+4.3}_{-5.2}$	$26.7^{+2.1}_{-1.7}$	$-0.09^{+0.18}_{-0.21}$	$59.8^{+4.8}_{-3.8}$	$0.67^{+0.07}_{-0.08}$	$2.7^{+0.5}_{-0.5}$	$3.4^{+0.5}_{-0.7}\times10^{56}$	1020^{+430}_{-360}	$0.20^{+0.07}_{-0.07}$	39
GW170823	$39.6^{+10.0}_{-6.6}$	$29.4^{+6.3}_{-7.1}$	$29.3^{+4.2}_{-3.2}$	$0.08^{+0.20}_{-0.22}$	$65.6^{+9.4}_{-6.6}$	$0.71^{+0.08}_{-0.10}$	$3.3^{+0.9}_{-0.8}$	$3.6^{+0.6}_{-0.9}\times10^{56}$	1850^{+840}_{-840}	$0.34^{+0.13}_{-0.14}$	1651

Abbott+19

E.M. search for BBH GW events

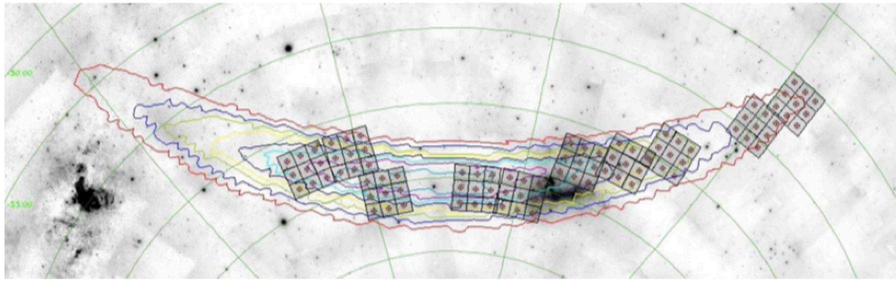

GW 150914: 630 deg^2 skymap
90 deg^2 observed with VST
(6 epochs between Sep 17 and Nov 18)

Brocato+16; Abbott+16

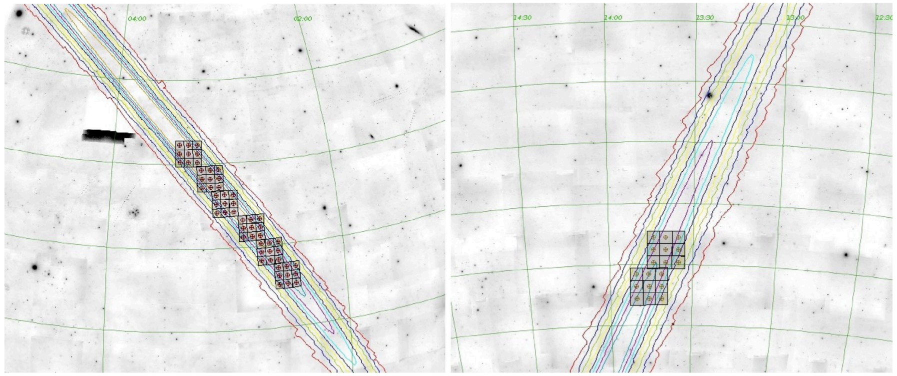

GW 151226: 1240 deg^2 skymap
72 deg^2 observed with VST
(6 epochs between Dec 27 and Feb 10)

Brocato+16

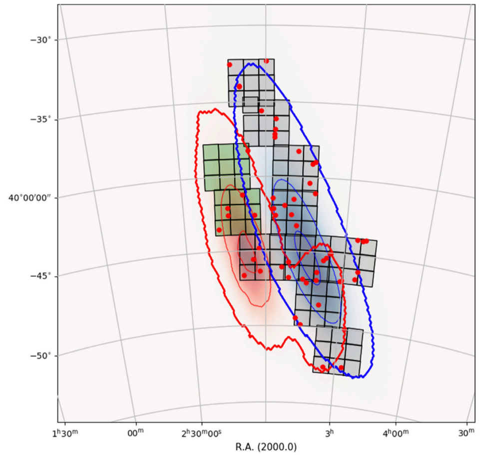

GW 170814: 87 deg^2 skymap
59% observed with VST
(6 epochs between Aug 14 and Sep 28)

Grado+20

Huge observational effort, mainly with wide-field facilities

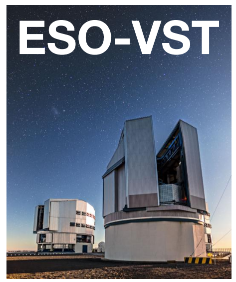

Several transients discovered
No EM counterpart found

Characterization of candidates with TNG

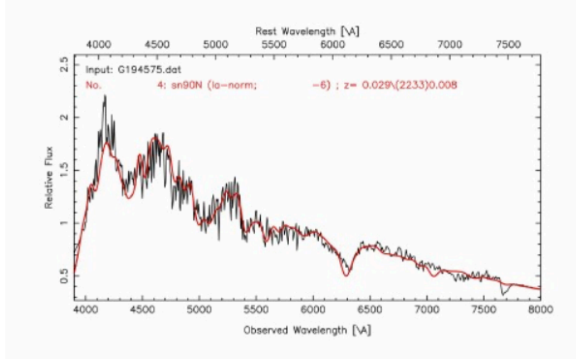

Figure 1: TNG spectrum of LSQ15bjb of 26 October 2015 (black) compared with that of SN 1990N (red), six days before *B*-band maximum light.

2015GCN.18536....1D2015
LIGO/Virgo G194575: **INAF-TNG** follow-up of iPTF15dkm and iPTF15dlj
D'Avanzo, P.; Melandri, A.; Piranomonte, S. and 28 more

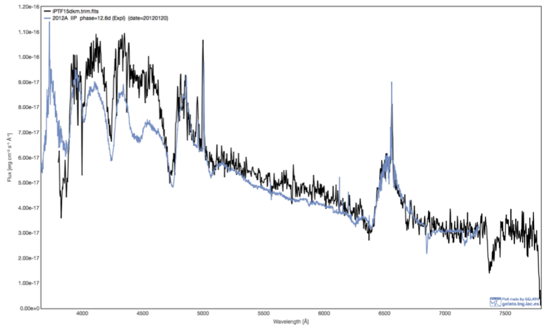

Figure 2: TNG spectrum of iPTF15dkm of 29 October 2015 (black) and best match with SN 2012A (blue), using GELATO (Harutyunyan et al. 2008, A&A, 488, 383).

2015GCN.18488....1P2015
LIGO/Virgo G194575: **INAF-TNG** spectra of LSQ15bjb
Piranomonte, S.; D'Avanzo, P.; Melandri, A. and 23 more

2015GCN.18476....1D2015
LIGO/Virgo G194575: **INAF-TNG** follow-up of LSQ15bjb
D'Avanzo, P.; Melandri, A.; Piranomonte, S. and 19 more

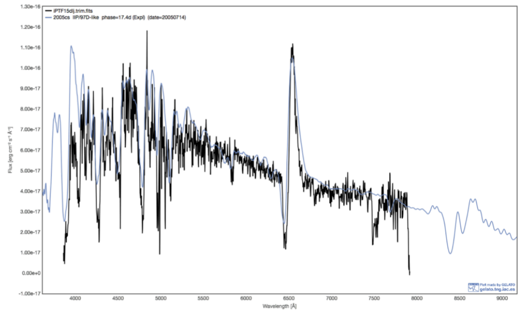

Figure 3: TNG spectrum of iPTF15dlj of 29 October 2015 (black) and best match with SN 2005cs (blue), using GELATO (Harutyunyan et al. 2008, A&A, 488, 383).

2015GCN.18775....1D2015
LIGO/Virgo G211117: **INAF TNG** follow-up of MASTER OT J020906.21+013800.1.
D'Avanzo, P.; Melandri, A.; Piranomonte, S. and 28 more

Characterization of candidates with TNG

iPTF15dld:
a low-luminosity, broad-line Ic supernova

Pian+17

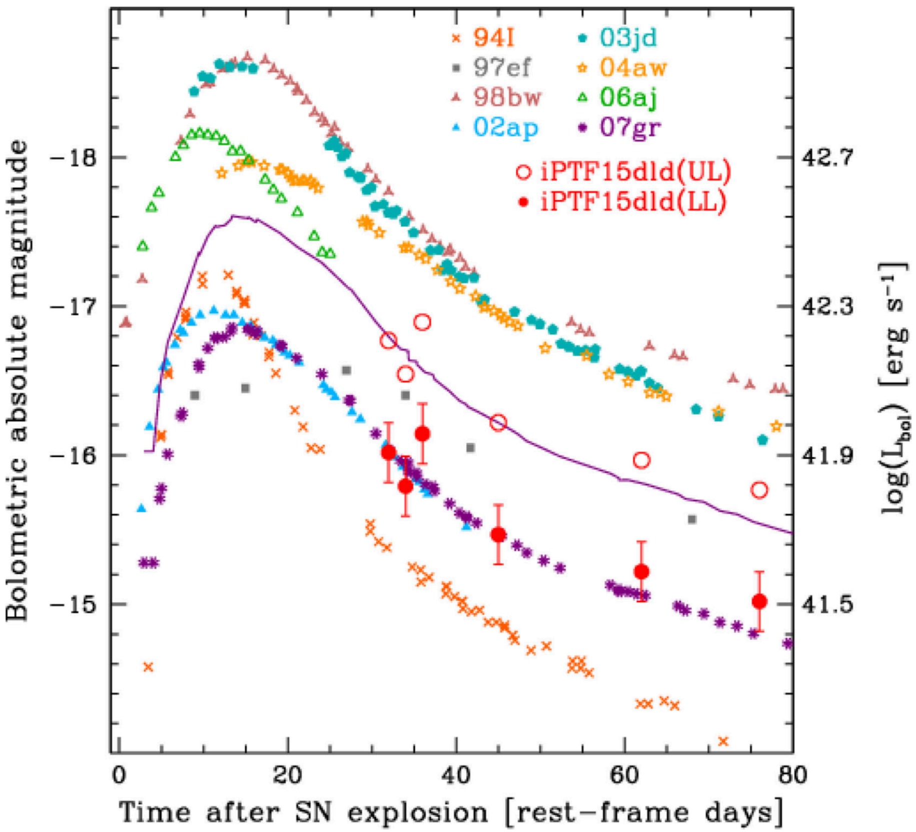

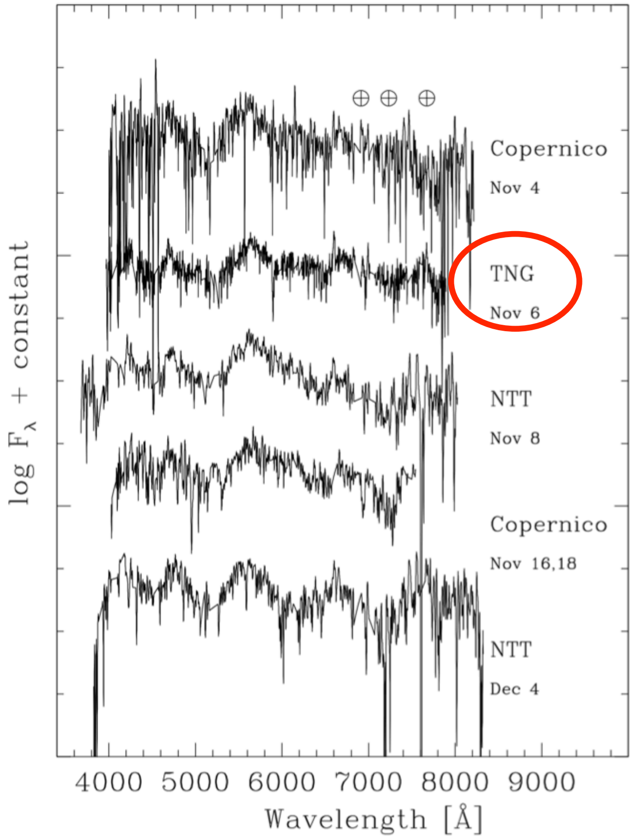

Characterization of candidates with TNG

ATLAS17aeu:
transient discovered during the search for the e.m. counterpart of GW 170104 (BBH). Likely associated with the long GRB 170105 (and associated SN) at z_ph ~ 0.5

Melandri+19

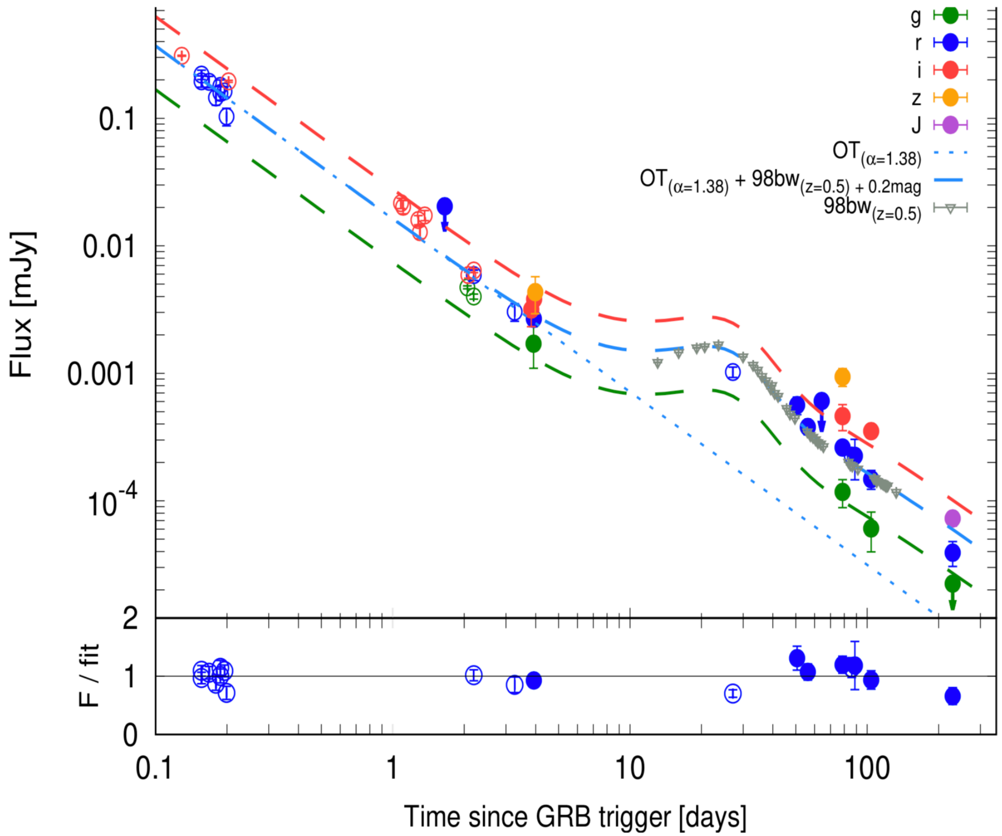

The GW era – O1 & O2

Sept 2015 – Jan 2016: LVC O1 science run
Nov 2016 – Aug 2017: LVC O2 science run

Event	$m_1/\mathrm{M}_\odot$	$m_2/\mathrm{M}_\odot$	$\mathcal{M}/\mathrm{M}_\odot$	χ_{eff}	$M_f/\mathrm{M}_\odot$	a_f	$E_{\mathrm{rad}}/(\mathrm{M}_\odot c^2)$	$\ell_{\mathrm{peak}}/(\mathrm{erg\,s^{-1}})$	d_L/Mpc	z	$\Delta\Omega/\mathrm{deg}^2$
GW150914	$35.6^{+4.8}_{-3.0}$	$30.6^{+3.0}_{-4.4}$	$28.6^{+1.6}_{-1.5}$	$-0.01^{+0.12}_{-0.13}$	$63.1^{+3.3}_{-3.0}$	$0.69^{+0.05}_{-0.04}$	$3.1^{+0.4}_{-0.4}$	$3.6^{+0.4}_{-0.4} \times 10^{56}$	430^{+150}_{-170}	$0.09^{+0.03}_{-0.03}$	180
GW151012	$23.3^{+14.0}_{-5.5}$	$13.6^{+4.1}_{-4.8}$	$15.2^{+2.0}_{-1.1}$	$0.04^{+0.28}_{-0.19}$	$35.7^{+9.9}_{-3.8}$	$0.67^{+0.13}_{-0.11}$	$1.5^{+0.5}_{-0.5}$	$3.2^{+0.8}_{-1.7} \times 10^{56}$	1060^{+540}_{-480}	$0.21^{+0.09}_{-0.09}$	1555
GW151226	$13.7^{+8.8}_{-3.2}$	$7.7^{+2.2}_{-2.6}$	$8.9^{+0.3}_{-0.3}$	$0.18^{+0.20}_{-0.12}$	$20.5^{+6.4}_{-1.5}$	$0.74^{+0.07}_{-0.05}$	$1.0^{+0.1}_{-0.2}$	$3.4^{+0.7}_{-1.7} \times 10^{56}$	440^{+180}_{-190}	$0.09^{+0.04}_{-0.04}$	1033
GW170104	$31.0^{+7.2}_{-5.6}$	$20.1^{+4.9}_{-4.5}$	$21.5^{+2.1}_{-1.7}$	$-0.04^{+0.17}_{-0.20}$	$49.1^{+5.2}_{-3.9}$	$0.66^{+0.08}_{-0.10}$	$2.2^{+0.5}_{-0.5}$	$3.3^{+0.6}_{-0.9} \times 10^{56}$	960^{+430}_{-410}	$0.19^{+0.07}_{-0.08}$	924
GW170608	$10.9^{+5.3}_{-1.7}$	$7.6^{+1.3}_{-2.1}$	$7.9^{+0.2}_{-0.2}$	$0.03^{+0.19}_{-0.07}$	$17.8^{+3.2}_{-0.7}$	$0.69^{+0.04}_{-0.04}$	$0.9^{+0.05}_{-0.1}$	$3.5^{+0.4}_{-1.3} \times 10^{56}$	320^{+120}_{-110}	$0.07^{+0.02}_{-0.02}$	396
GW170729	$50.6^{+16.6}_{-10.2}$	$34.3^{+9.1}_{-10.1}$	$35.7^{+6.5}_{-4.7}$	$0.36^{+0.21}_{-0.25}$	$80.3^{+14.6}_{-10.2}$	$0.81^{+0.07}_{-0.13}$	$4.8^{+1.7}_{-1.7}$	$4.2^{+0.9}_{-1.5} \times 10^{56}$	2750^{+1350}_{-1320}	$0.48^{+0.19}_{-0.20}$	1033
GW170809	$35.2^{+8.3}_{-6.0}$	$23.8^{+5.2}_{-5.1}$	$25.0^{+2.1}_{-1.6}$	$0.07^{+0.16}_{-0.16}$	$56.4^{+5.2}_{-3.7}$	$0.70^{+0.08}_{-0.09}$	$2.7^{+0.6}_{-0.6}$	$3.5^{+0.6}_{-0.9} \times 10^{56}$	990^{+320}_{-380}	$0.20^{+0.05}_{-0.07}$	340
GW170814	$30.7^{+5.7}_{-3.0}$	$25.3^{+2.9}_{-4.1}$	$24.2^{+1.4}_{-1.1}$	$0.07^{+0.12}_{-0.11}$	$53.4^{+3.2}_{-2.4}$	$0.72^{+0.07}_{-0.05}$	$2.7^{+0.4}_{-0.3}$	$3.7^{+0.4}_{-0.5} \times 10^{56}$	580^{+160}_{-210}	$0.12^{+0.03}_{-0.04}$	87
GW170817	$1.46^{+0.12}_{-0.10}$	$1.27^{+0.09}_{-0.09}$	$1.186^{+0.001}_{-0.001}$	$0.00^{+0.02}_{-0.01}$	≤ 2.8	≤ 0.89	≥ 0.04	$\geq 0.1 \times 10^{56}$	40^{+10}_{-10}	$0.01^{+0.00}_{-0.00}$	16
GW170818	$35.5^{+7.5}_{-4.7}$	$26.8^{+4.3}_{-5.2}$	$26.7^{+2.1}_{-1.7}$	$-0.09^{+0.18}_{-0.21}$	$59.8^{+4.8}_{-3.8}$	$0.67^{+0.07}_{-0.08}$	$2.7^{+0.5}_{-0.5}$	$3.4^{+0.5}_{-0.7} \times 10^{56}$	1020^{+430}_{-360}	$0.20^{+0.07}_{-0.07}$	39
GW170823	$39.6^{+10.0}_{-6.6}$	$29.4^{+6.3}_{-7.1}$	$29.3^{+4.2}_{-3.2}$	$0.08^{+0.20}_{-0.22}$	$65.6^{+9.4}_{-6.6}$	$0.71^{+0.08}_{-0.10}$	$3.3^{+0.9}_{-0.8}$	$3.6^{+0.6}_{-0.9} \times 10^{56}$	1850^{+840}_{-840}	$0.34^{+0.13}_{-0.14}$	1651

Abbott+19

The GW era – O1 & O2

Sept 2015 – Jan 2016: LVC O1 science run
Nov 2016 – Aug 2017: LVC O2 science run

Event	$m_1/\mathrm{M}_\odot$	$m_2/\mathrm{M}_\odot$	$\mathcal{M}/\mathrm{M}_\odot$	χ_{eff}	$M_{\mathrm{f}}/\mathrm{M}_\odot$	a_{f}	$E_{\mathrm{rad}}/(\mathrm{M}_\odot c^2)$	$\ell_{\mathrm{peak}}/(\mathrm{erg\,s^{-1}})$	d_L/Mpc	z	$\Delta\Omega/\mathrm{deg}^2$
GW150914	$35.6^{+4.8}_{-3.0}$	$30.6^{+3.0}_{-4.4}$	$28.6^{+1.6}_{-1.5}$	$-0.01^{+0.12}_{-0.13}$	$63.1^{+3.3}_{-3.0}$	$0.69^{+0.05}_{-0.04}$	$3.1^{+0.4}_{-0.4}$	$3.6^{+0.4}_{-0.4} \times 10^{56}$	430^{+150}_{-170}	$0.09^{+0.03}_{-0.03}$	180
GW151012	$23.3^{+14.0}_{-5.5}$	$13.6^{+4.1}_{-4.8}$	$15.2^{+2.0}_{-1.1}$	$0.04^{+0.28}_{-0.19}$	$35.7^{+9.9}_{-3.8}$	$0.67^{+0.13}_{-0.11}$	$1.5^{+0.5}_{-0.5}$	$3.2^{+0.8}_{-1.7} \times 10^{56}$	1060^{+540}_{-480}	$0.21^{+0.09}_{-0.09}$	1555
GW151226	$13.7^{+8.8}_{-3.2}$	$7.7^{+2.2}_{-2.6}$	$8.9^{+0.3}_{-0.3}$	$0.18^{+0.20}_{-0.12}$	$20.5^{+6.4}_{-1.5}$	$0.74^{+0.07}_{-0.05}$	$1.0^{+0.1}_{-0.2}$	$3.4^{+0.7}_{-1.7} \times 10^{56}$	440^{+180}_{-190}	$0.09^{+0.04}_{-0.04}$	1033
GW170104	$31.0^{+7.2}_{-5.6}$	$20.1^{+4.9}_{-4.5}$	$21.5^{+2.1}_{-1.7}$	$-0.04^{+0.17}_{-0.20}$	$49.1^{+5.2}_{-3.9}$	$0.66^{+0.08}_{-0.10}$	$2.2^{+0.5}_{-0.5}$	$3.3^{+0.6}_{-0.9} \times 10^{56}$	960^{+430}_{-410}	$0.19^{+0.07}_{-0.08}$	924
GW170608	$10.9^{+5.3}_{-1.7}$	$7.6^{+1.3}_{-2.1}$	$7.9^{+0.2}_{-0.2}$	$0.03^{+0.19}_{-0.07}$	$17.8^{+3.2}_{-0.7}$	$0.69^{+0.04}_{-0.04}$	$0.9^{+0.05}_{-0.1}$	$3.5^{+0.4}_{-1.3} \times 10^{56}$	320^{+120}_{-110}	$0.07^{+0.02}_{-0.02}$	396
GW170729	$50.6^{+16.6}_{-10.2}$	$34.3^{+9.1}_{-10.1}$	$35.7^{+6.5}_{-4.7}$	$0.36^{+0.21}_{-0.25}$	$80.3^{+14.6}_{-10.2}$	$0.81^{+0.07}_{-0.13}$	$4.8^{+1.7}_{-1.7}$	$4.2^{+0.9}_{-1.5} \times 10^{56}$	2750^{+1350}_{-1320}	$0.48^{+0.19}_{-0.20}$	1033
GW170809	$35.2^{+8.3}_{-6.0}$	$23.8^{+5.2}_{-5.1}$	$25.0^{+2.1}_{-1.6}$	$0.07^{+0.16}_{-0.16}$	$56.4^{+5.2}_{-3.7}$	$0.70^{+0.08}_{-0.09}$	$2.7^{+0.6}_{-0.6}$	$3.5^{+0.6}_{-0.9} \times 10^{56}$	990^{+320}_{-380}	$0.20^{+0.05}_{-0.07}$	340
GW170814	$30.7^{+5.7}_{-3.0}$	$25.3^{+2.9}_{-4.1}$	$24.2^{+1.4}_{-1.1}$	$0.07^{+0.12}_{-0.11}$	$53.4^{+3.2}_{-2.4}$	$0.72^{+0.07}_{-0.05}$	$2.7^{+0.4}_{-0.3}$	$3.7^{+0.4}_{-0.5} \times 10^{56}$	580^{+160}_{-210}	$0.12^{+0.03}_{-0.04}$	87
GW170817	$1.46^{+0.12}_{-0.10}$	$1.27^{+0.09}_{-0.09}$	$1.186^{+0.001}_{-0.001}$	$0.00^{+0.02}_{-0.01}$	≤ 2.8	≤ 0.89	≥ 0.04	$\geq 0.1 \times 10^{56}$	40^{+10}_{-10}	$0.01^{+0.00}_{-0.00}$	16
GW170818	$35.5^{+7.5}_{-4.7}$	$26.8^{+4.3}_{-5.2}$	$26.7^{+2.1}_{-1.7}$	$-0.09^{+0.18}_{-0.21}$	$59.8^{+4.8}_{-3.8}$	$0.67^{+0.07}_{-0.08}$	$2.7^{+0.5}_{-0.5}$	$3.4^{+0.5}_{-0.7} \times 10^{56}$	1020^{+430}_{-360}	$0.20^{+0.07}_{-0.07}$	39
GW170823	$39.6^{+10.0}_{-6.6}$	$29.4^{+6.3}_{-7.1}$	$29.3^{+4.2}_{-3.2}$	$0.08^{+0.20}_{-0.22}$	$65.6^{+9.4}_{-6.6}$	$0.71^{+0.08}_{-0.10}$	$3.3^{+0.9}_{-0.8}$	$3.6^{+0.6}_{-0.9} \times 10^{56}$	1850^{+840}_{-840}	$0.34^{+0.13}_{-0.14}$	1651

Abbott+19

GW 170817 / AT2017gfo / GRB 170817A

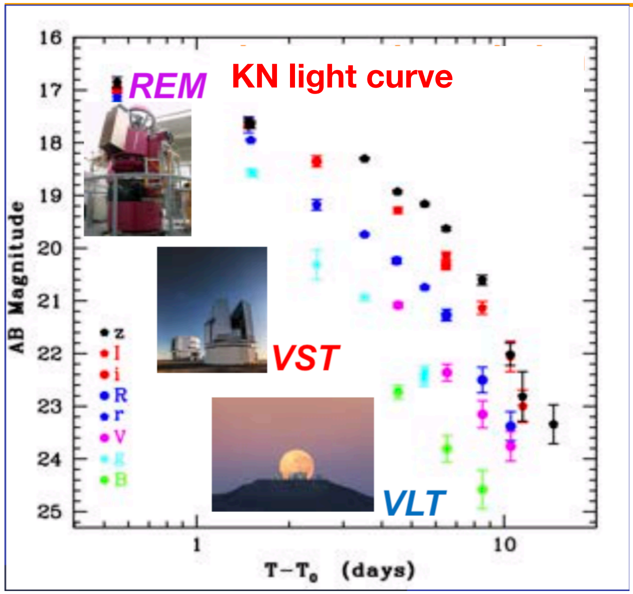

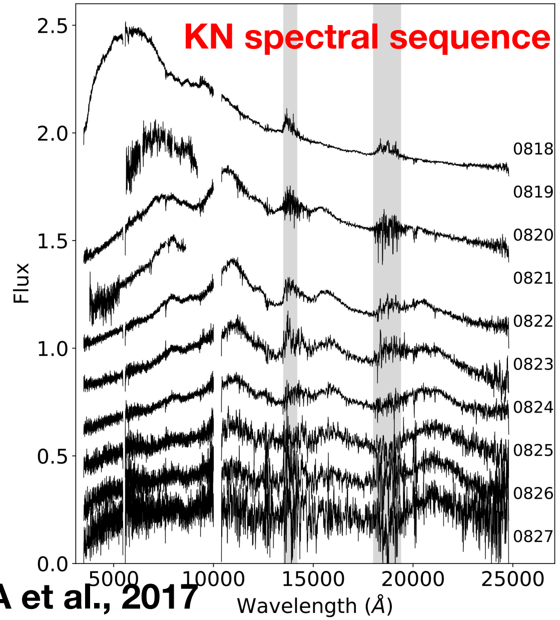

Pian, PDA et al., 2017

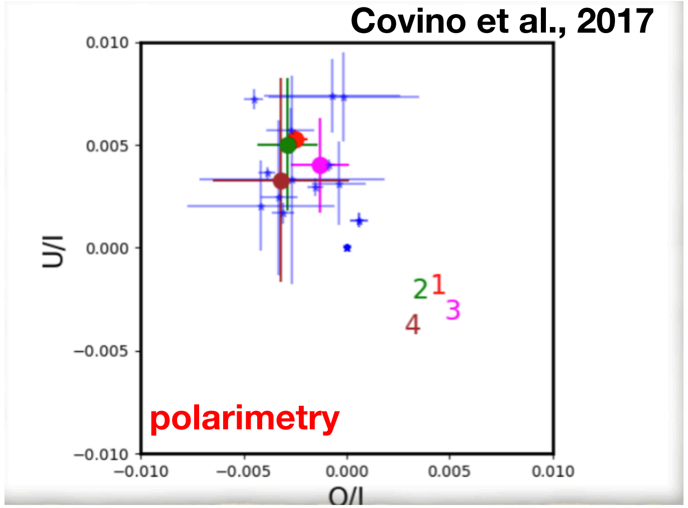

Full characterization of the KN and GRB properties

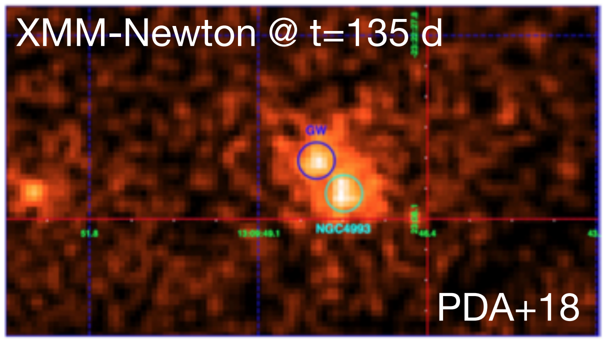

detection of the afterglow at the peak

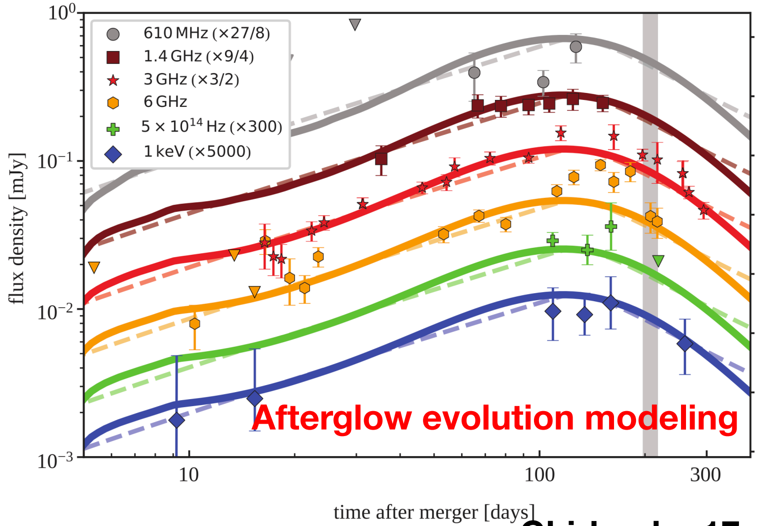

Ghirlanda+17

Evidence for a structured GRB jet

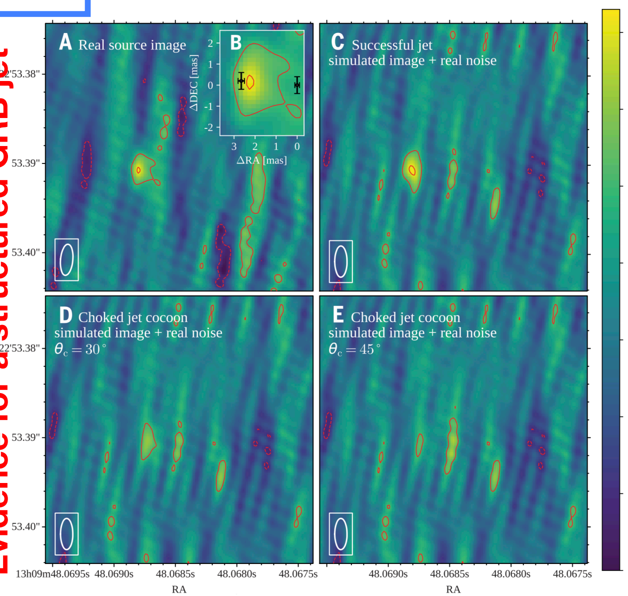

The GW era – O3


LIGO Hanford
LIGO Livingston
GEO 600
Virgo
KAGRA
LIGO-India

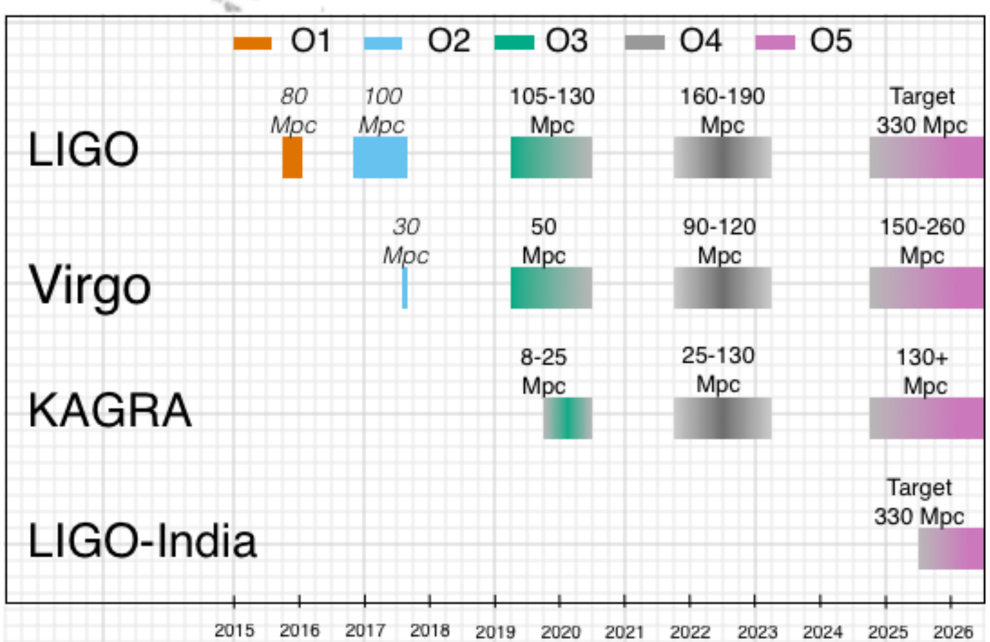
O1
O2
O3
O4
O5
LIGO
80 Mpc
100 Mpc
105-130 Mpc
160-190 Mpc
Target 330 Mpc
Virgo
30 Mpc
50 Mpc
90-120 Mpc
150-260 Mpc
KAGRA
8-25 Mpc
25-130 Mpc
130+ Mpc
LIGO-India
Target 330 Mpc
2015
2016
2017
2018
2019
2020
2021
2022
2023
2024
2025
2026

EM follow-up: ready for O3

Search (& follow-up) European teams

www.engrave-eso.org

Governing Council: M. Branchesi, **E. Brocato**, **P. D'Avanzo**, J. Hjorth, P. Jonker, E. Pian, S. Smartt (Chair), J. Sollerman, D. Steeghs, N. Tanvir.
Executive Committee: A. Levan (Chair), M. Fraser, K. Maguire, D. Malesani, **O. S. Salafia,** S. Vergani.

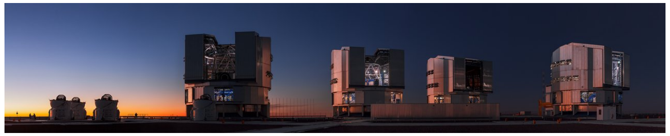

A collaboration of ~ 200 ESO scientists
Approved program during Oct 2018 – Mar 2020 fully covering O3. Time for EM counterparts **follow-up** on every useful **VLT** instrument + **ALMA HST** and **JWST**.

www.grawita.inaf.it

www.star.le.ac.uk/nrt3/VINROUGE/

The **G**W **O**ptical
Transient **O**bserver
GOTO
www.goto-observatory.org

www.pessto.org

The GW era – O3

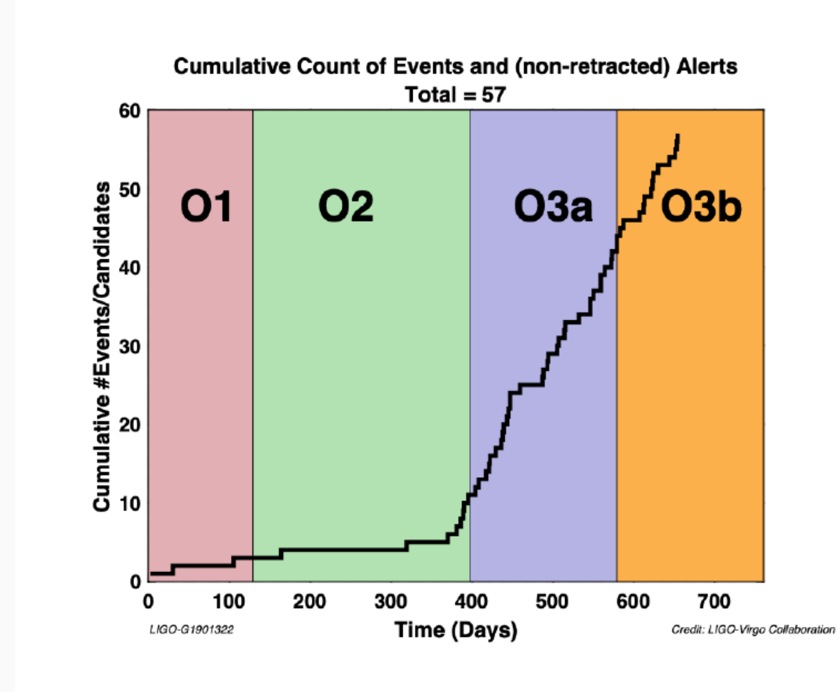

Cumulative Count of Events and (non-retracted) Alerts
Total = 57
Cumulative #Events/Candidates
O1
O2
O3a
O3b
0
10
20
30
40
50
60
0
100
200
300
400
500
600
700
Time (Days)
LIGO-G1901322
Credit: LIGO-Virgo Collaboration

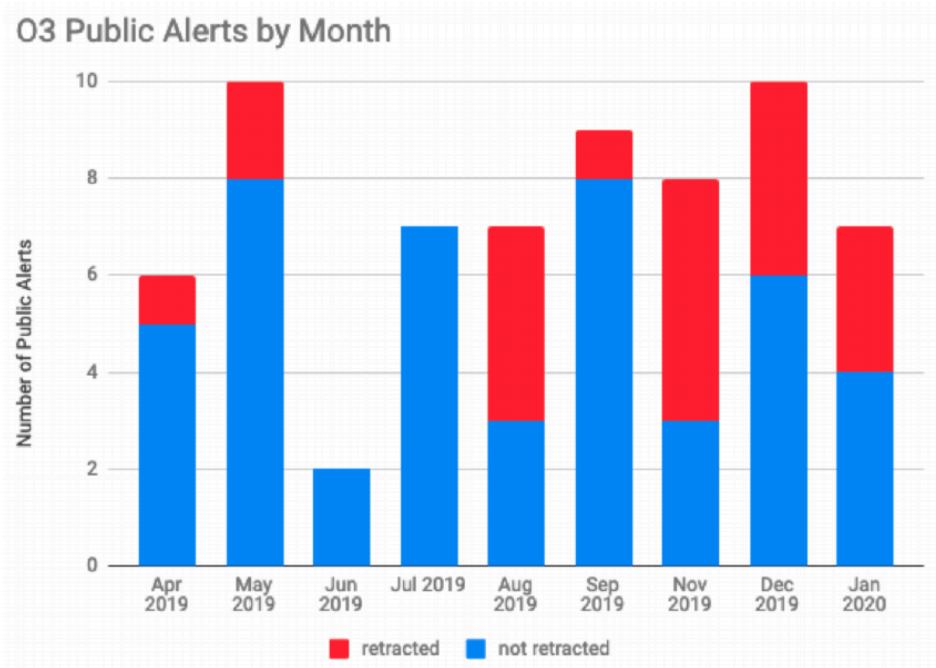

O3 Public Alerts by Month
Number of Public Alerts
0
2
4
6
8
10
Apr 2019
May 2019
Jun 2019
Jul 2019
Aug 2019
Sep 2019
Nov 2019
Dec 2019
Jan 2020
retracted
not retracted

The GW era – O3a

Event	M ($M_\odot$)	$\mathcal{M}$ ($M_\odot$)	m_1 ($M_\odot$)	m_2 ($M_\odot$)	χ_{eff}	D_L (Gpc)	z	M_f ($M_\odot$)	χ_f	$\Delta\Omega$ (deg^2)	SNR
GW190408_181802	$43.0^{+4.2}_{-3.0}$	$18.3^{+1.9}_{-1.2}$	$24.6^{+5.1}_{-3.4}$	$18.4^{+3.3}_{-3.6}$	$-0.03^{+0.14}_{-0.19}$	$1.55^{+0.40}_{-0.60}$	$0.29^{+0.06}_{-0.10}$	$41.1^{+3.9}_{-2.8}$	$0.67^{+0.06}_{-0.07}$	150	$15.3^{+0.2}_{-0.3}$
GW190412	$38.4^{+3.8}_{-3.7}$	$13.3^{+0.4}_{-0.3}$	$30.1^{+4.7}_{-5.1}$	$8.3^{+1.6}_{-0.9}$	$0.25^{+0.08}_{-0.11}$	$0.74^{+0.14}_{-0.17}$	$0.15^{+0.03}_{-0.03}$	$37.3^{+3.9}_{-3.8}$	$0.67^{+0.05}_{-0.06}$	21	$18.9^{+0.2}_{-0.3}$
GW190413_052954	$58.6^{+13.3}_{-9.7}$	$24.6^{+5.5}_{-4.1}$	$34.7^{+12.6}_{-8.1}$	$23.7^{+7.3}_{-6.7}$	$-0.01^{+0.29}_{-0.34}$	$3.55^{+2.27}_{-1.66}$	$0.59^{+0.29}_{-0.24}$	$56.0^{+12.5}_{-9.2}$	$0.68^{+0.12}_{-0.13}$	1500	$8.9^{+0.4}_{-0.7}$
GW190413_134308	$78.8^{+17.4}_{-11.9}$	$33.0^{+8.2}_{-5.4}$	$47.5^{+13.5}_{-10.7}$	$31.8^{+11.7}_{-10.8}$	$-0.03^{+0.25}_{-0.29}$	$4.45^{+2.48}_{-2.12}$	$0.71^{+0.31}_{-0.30}$	$75.5^{+16.4}_{-11.4}$	$0.68^{+0.10}_{-0.12}$	730	$10.0^{+0.4}_{-0.5}$
GW190421_213856	$72.9^{+13.4}_{-9.2}$	$31.2^{+5.9}_{-4.2}$	$41.3^{+10.4}_{-6.9}$	$31.9^{+8.0}_{-8.8}$	$-0.06^{+0.22}_{-0.27}$	$2.88^{+1.37}_{-1.38}$	$0.49^{+0.19}_{-0.21}$	$69.7^{+12.5}_{-8.7}$	$0.67^{+0.10}_{-0.11}$	1200	$10.7^{+0.2}_{-0.4}$
GW190424_180648	$72.6^{+13.3}_{-10.7}$	$31.0^{+5.8}_{-4.6}$	$40.5^{+11.1}_{-7.3}$	$31.8^{+7.6}_{-7.7}$	$0.13^{+0.22}_{-0.22}$	$2.20^{+1.58}_{-1.16}$	$0.39^{+0.23}_{-0.19}$	$68.9^{+12.4}_{-10.1}$	$0.74^{+0.09}_{-0.09}$	28000	$10.4^{+0.2}_{-0.4}$
GW190425	$3.4^{+0.3}_{-0.1}$	$1.44^{+0.02}_{-0.02}$	$2.0^{+0.6}_{-0.3}$	$1.4^{+0.3}_{-0.3}$	$0.06^{+0.11}_{-0.05}$	$0.16^{+0.07}_{-0.07}$	$0.03^{+0.01}_{-0.02}$	–	–	10000	$12.4^{+0.3}_{-0.4}$
GW190426_152155	$7.2^{+3.5}_{-1.5}$	$2.41^{+0.08}_{-0.08}$	$5.7^{+3.9}_{-2.3}$	$1.5^{+0.8}_{-0.5}$	$-0.03^{+0.32}_{-0.30}$	$0.37^{+0.18}_{-0.16}$	$0.08^{+0.04}_{-0.03}$	–	–	1300	$8.7^{+0.5}_{-0.6}$
GW190503_185404	$71.7^{+9.4}_{-8.3}$	$30.2^{+4.2}_{-4.2}$	$43.3^{+9.2}_{-8.1}$	$28.4^{+7.7}_{-8.0}$	$-0.03^{+0.20}_{-0.26}$	$1.45^{+0.69}_{-0.63}$	$0.27^{+0.11}_{-0.11}$	$68.6^{+8.8}_{-7.7}$	$0.66^{+0.09}_{-0.12}$	94	$12.4^{+0.2}_{-0.3}$
GW190512_180714	$35.9^{+3.8}_{-3.5}$	$14.6^{+1.3}_{-1.0}$	$23.3^{+5.3}_{-5.8}$	$12.6^{+3.6}_{-2.5}$	$0.03^{+0.12}_{-0.13}$	$1.43^{+0.55}_{-0.55}$	$0.27^{+0.09}_{-0.10}$	$34.5^{+3.8}_{-3.5}$	$0.65^{+0.07}_{-0.07}$	220	$12.2^{+0.2}_{-0.4}$
GW190513_205428	$53.9^{+8.6}_{-5.9}$	$21.6^{+3.8}_{-1.9}$	$35.7^{+9.5}_{-9.2}$	$18.0^{+7.7}_{-4.1}$	$0.11^{+0.28}_{-0.17}$	$2.06^{+0.88}_{-0.80}$	$0.37^{+0.13}_{-0.13}$	$51.6^{+8.2}_{-5.8}$	$0.68^{+0.14}_{-0.12}$	520	$12.9^{+0.3}_{-0.4}$
GW190514_065416	$67.2^{+18.7}_{-10.8}$	$28.5^{+7.9}_{-4.8}$	$39.0^{+14.7}_{-8.2}$	$28.4^{+9.3}_{-8.8}$	$-0.19^{+0.29}_{-0.32}$	$4.13^{+2.65}_{-2.17}$	$0.67^{+0.33}_{-0.31}$	$64.5^{+17.9}_{-10.4}$	$0.63^{+0.11}_{-0.15}$	3000	$8.2^{+0.3}_{-0.6}$
GW190517_055101	$63.5^{+9.6}_{-9.6}$	$26.6^{+4.0}_{-4.0}$	$37.4^{+11.7}_{-7.6}$	$25.3^{+7.0}_{-7.3}$	$0.52^{+0.19}_{-0.19}$	$1.86^{+1.62}_{-0.84}$	$0.34^{+0.24}_{-0.14}$	$59.3^{+9.1}_{-8.9}$	$0.87^{+0.05}_{-0.07}$	470	$10.7^{+0.4}_{-0.6}$
GW190519_153544	$106.6^{+13.5}_{-14.8}$	$44.5^{+6.4}_{-7.1}$	$66.0^{+10.7}_{-12.0}$	$40.5^{+11.0}_{-11.1}$	$0.31^{+0.20}_{-0.22}$	$2.53^{+1.83}_{-0.92}$	$0.44^{+0.25}_{-0.14}$	$101.0^{+12.4}_{-13.8}$	$0.79^{+0.07}_{-0.13}$	860	$15.6^{+0.2}_{-0.3}$
GW190521	$163.9^{+39.2}_{-23.5}$	$69.2^{+17.0}_{-10.6}$	$95.3^{+28.7}_{-18.9}$	$69.0^{+22.7}_{-23.1}$	$0.03^{+0.32}_{-0.39}$	$3.92^{+2.19}_{-1.95}$	$0.64^{+0.28}_{-0.28}$	$156.3^{+36.8}_{-22.4}$	$0.71^{+0.12}_{-0.16}$	1000	$14.2^{+0.3}_{-0.3}$
GW190521_074359	$74.7^{+7.0}_{-4.8}$	$32.1^{+3.2}_{-2.5}$	$42.2^{+5.9}_{-4.8}$	$32.8^{+5.4}_{-6.4}$	$0.09^{+0.10}_{-0.13}$	$1.24^{+0.40}_{-0.57}$	$0.24^{+0.07}_{-0.10}$	$71.0^{+6.5}_{-4.4}$	$0.72^{+0.05}_{-0.07}$	550	$25.8^{+0.1}_{-0.2}$
GW190527_092055	$59.1^{+21.3}_{-9.8}$	$24.3^{+9.1}_{-4.2}$	$36.5^{+16.4}_{-9.0}$	$22.6^{+10.5}_{-8.1}$	$0.11^{+0.28}_{-0.28}$	$2.49^{+2.48}_{-1.24}$	$0.44^{+0.34}_{-0.20}$	$56.4^{+20.2}_{-9.3}$	$0.71^{+0.12}_{-0.16}$	3700	$8.1^{+0.3}_{-0.9}$
GW190602_175927	$116.3^{+19.0}_{-15.6}$	$49.1^{+9.1}_{-8.5}$	$69.1^{+15.7}_{-13.0}$	$47.8^{+14.3}_{-17.4}$	$0.07^{+0.25}_{-0.24}$	$2.69^{+1.79}_{-1.12}$	$0.47^{+0.25}_{-0.17}$	$110.9^{+17.7}_{-14.9}$	$0.70^{+0.10}_{-0.14}$	690	$12.8^{+0.2}_{-0.3}$
GW190620_030421	$92.1^{+18.5}_{-13.1}$	$38.3^{+8.3}_{-6.5}$	$57.1^{+16.0}_{-12.7}$	$35.5^{+12.2}_{-12.3}$	$0.33^{+0.22}_{-0.25}$	$2.81^{+1.68}_{-1.31}$	$0.49^{+0.23}_{-0.20}$	$87.2^{+16.8}_{-12.1}$	$0.79^{+0.08}_{-0.15}$	7200	$12.1^{+0.3}_{-0.4}$
GW190630_185205	$59.1^{+4.6}_{-4.8}$	$24.9^{+2.1}_{-2.1}$	$35.1^{+6.9}_{-5.6}$	$23.7^{+5.2}_{-5.1}$	$0.10^{+0.12}_{-0.13}$	$0.89^{+0.56}_{-0.37}$	$0.18^{+0.10}_{-0.07}$	$56.4^{+4.4}_{-4.6}$	$0.70^{+0.05}_{-0.07}$	1200	$15.6^{+0.2}_{-0.3}$
GW190701_203306	$94.3^{+12.1}_{-9.5}$	$40.3^{+5.4}_{-4.9}$	$53.9^{+11.8}_{-8.0}$	$40.8^{+8.7}_{-12.0}$	$-0.07^{+0.23}_{-0.29}$	$2.06^{+0.76}_{-0.73}$	$0.37^{+0.11}_{-0.12}$	$90.2^{+11.3}_{-8.9}$	$0.66^{+0.09}_{-0.13}$	46	$11.3^{+0.2}_{-0.3}$
GW190706_222641	$104.1^{+20.2}_{-13.9}$	$42.7^{+10.0}_{-7.0}$	$67.0^{+14.6}_{-16.2}$	$38.2^{+14.6}_{-13.3}$	$0.28^{+0.26}_{-0.29}$	$4.42^{+2.59}_{-1.93}$	$0.71^{+0.32}_{-0.27}$	$99.0^{+18.3}_{-13.5}$	$0.78^{+0.09}_{-0.18}$	650	$12.6^{+0.2}_{-0.4}$
GW190707_093326	$20.1^{+1.9}_{-1.3}$	$8.5^{+0.6}_{-0.5}$	$11.6^{+3.3}_{-1.7}$	$8.4^{+1.4}_{-1.7}$	$-0.05^{+0.10}_{-0.08}$	$0.77^{+0.38}_{-0.37}$	$0.16^{+0.07}_{-0.07}$	$19.2^{+1.9}_{-1.3}$	$0.66^{+0.03}_{-0.04}$	1300	$13.3^{+0.2}_{-0.4}$
GW190708_232457	$30.9^{+2.5}_{-1.8}$	$13.2^{+0.9}_{-0.6}$	$17.6^{+4.7}_{-2.3}$	$13.2^{+2.0}_{-2.7}$	$0.02^{+0.10}_{-0.08}$	$0.88^{+0.33}_{-0.39}$	$0.18^{+0.06}_{-0.07}$	$29.5^{+2.5}_{-1.8}$	$0.69^{+0.04}_{-0.04}$	14000	$13.1^{+0.2}_{-0.3}$
GW190719_215514	$57.8^{+18.3}_{-10.7}$	$23.5^{+6.5}_{-4.0}$	$36.5^{+18.0}_{-10.3}$	$20.8^{+9.0}_{-7.2}$	$0.32^{+0.29}_{-0.31}$	$3.94^{+2.59}_{-2.00}$	$0.64^{+0.33}_{-0.29}$	$54.9^{+17.3}_{-10.2}$	$0.78^{+0.11}_{-0.17}$	2900	$8.3^{+0.3}_{-0.8}$
GW190720_000836	$21.5^{+4.3}_{-2.3}$	$8.9^{+0.5}_{-0.8}$	$13.4^{+6.7}_{-3.0}$	$7.8^{+2.3}_{-2.2}$	$0.18^{+0.14}_{-0.12}$	$0.79^{+0.69}_{-0.32}$	$0.16^{+0.12}_{-0.06}$	$20.4^{+4.5}_{-2.2}$	$0.72^{+0.06}_{-0.05}$	460	$11.0^{+0.3}_{-0.7}$
GW190727_060333	$67.1^{+11.7}_{-8.0}$	$28.6^{+5.3}_{-3.7}$	$38.0^{+9.5}_{-6.2}$	$29.4^{+7.1}_{-8.4}$	$0.11^{+0.26}_{-0.25}$	$3.30^{+1.54}_{-1.50}$	$0.55^{+0.21}_{-0.22}$	$63.8^{+10.9}_{-7.5}$	$0.73^{+0.10}_{-0.10}$	830	$11.9^{+0.3}_{-0.5}$
GW190728_064510	$20.6^{+4.5}_{-1.3}$	$8.6^{+0.5}_{-0.3}$	$12.3^{+7.2}_{-2.2}$	$8.1^{+1.7}_{-2.6}$	$0.12^{+0.20}_{-0.07}$	$0.87^{+0.26}_{-0.37}$	$0.18^{+0.05}_{-0.07}$	$19.6^{+4.7}_{-1.3}$	$0.71^{+0.04}_{-0.04}$	400	$13.0^{+0.2}_{-0.4}$
GW190731_140936	$70.1^{+15.8}_{-11.3}$	$29.5^{+7.1}_{-5.2}$	$41.5^{+12.2}_{-9.0}$	$28.8^{+9.7}_{-9.5}$	$0.06^{+0.24}_{-0.24}$	$3.30^{+2.39}_{-1.72}$	$0.55^{+0.31}_{-0.26}$	$67.0^{+14.6}_{-10.8}$	$0.70^{+0.10}_{-0.13}$	3400	$8.7^{+0.2}_{-0.5}$
GW190803_022701	$64.5^{+12.6}_{-9.0}$	$27.3^{+5.7}_{-4.1}$	$37.3^{+10.6}_{-7.0}$	$27.3^{+7.8}_{-8.2}$	$-0.03^{+0.24}_{-0.27}$	$3.27^{+1.95}_{-1.58}$	$0.55^{+0.26}_{-0.24}$	$61.7^{+11.8}_{-8.5}$	$0.68^{+0.10}_{-0.11}$	1500	$8.6^{+0.3}_{-0.5}$
GW190814	$25.8^{+1.0}_{-0.9}$	$6.09^{+0.06}_{-0.06}$	$23.2^{+1.1}_{-1.0}$	$2.59^{+0.08}_{-0.09}$	$0.00^{+0.06}_{-0.06}$	$0.24^{+0.04}_{-0.05}$	$0.05^{+0.009}_{-0.010}$	$25.6^{+1.1}_{-0.9}$	$0.28^{+0.02}_{-0.02}$	19	$24.9^{+0.1}_{-0.2}$
GW190828_063405	$58.0^{+7.7}_{-4.8}$	$25.0^{+3.4}_{-2.1}$	$32.1^{+5.8}_{-4.0}$	$26.2^{+4.6}_{-4.8}$	$0.19^{+0.15}_{-0.16}$	$2.13^{+0.66}_{-0.93}$	$0.38^{+0.10}_{-0.15}$	$54.9^{+7.2}_{-4.3}$	$0.75^{+0.06}_{-0.07}$	520	$16.2^{+0.2}_{-0.3}$
GW190828_065509	$34.4^{+5.4}_{-4.4}$	$13.3^{+1.2}_{-1.0}$	$24.1^{+7.0}_{-7.2}$	$10.2^{+3.6}_{-2.1}$	$0.08^{+0.16}_{-0.16}$	$1.60^{+0.62}_{-0.60}$	$0.30^{+0.10}_{-0.10}$	$33.1^{+5.5}_{-4.5}$	$0.65^{+0.08}_{-0.08}$	660	$10.0^{+0.3}_{-0.5}$
GW190909_114149	$75.0^{+55.9}_{-17.6}$	$30.9^{+17.2}_{-7.5}$	$45.8^{+52.7}_{-13.3}$	$28.3^{+13.4}_{-12.7}$	$-0.06^{+0.37}_{-0.36}$	$3.77^{+3.27}_{-2.22}$	$0.62^{+0.41}_{-0.33}$	$72.0^{+54.9}_{-16.8}$	$0.66^{+0.15}_{-0.20}$	4700	$8.1^{+0.4}_{-0.6}$
GW190910_112807	$79.6^{+9.3}_{-9.1}$	$34.3^{+4.1}_{-4.1}$	$43.9^{+7.6}_{-6.1}$	$35.6^{+6.3}_{-7.2}$	$0.02^{+0.18}_{-0.18}$	$1.46^{+1.03}_{-0.58}$	$0.28^{+0.16}_{-0.10}$	$75.8^{+8.5}_{-8.6}$	$0.70^{+0.08}_{-0.07}$	11000	$14.1^{+0.2}_{-0.3}$
GW190915_235702	$59.9^{+7.5}_{-6.4}$	$25.3^{+3.2}_{-2.7}$	$35.3^{+9.5}_{-6.4}$	$24.4^{+5.6}_{-6.1}$	$0.02^{+0.20}_{-0.25}$	$1.62^{+0.71}_{-0.61}$	$0.30^{+0.11}_{-0.10}$	$57.2^{+7.1}_{-6.0}$	$0.70^{+0.09}_{-0.11}$	400	$13.6^{+0.2}_{-0.3}$
GW190924_021846	$13.9^{+5.1}_{-1.0}$	$5.8^{+0.2}_{-0.2}$	$8.9^{+7.0}_{-2.0}$	$5.0^{+1.4}_{-1.9}$	$0.03^{+0.30}_{-0.09}$	$0.57^{+0.22}_{-0.22}$	$0.12^{+0.04}_{-0.04}$	$13.3^{+5.2}_{-1.0}$	$0.67^{+0.05}_{-0.05}$	360	$11.5^{+0.3}_{-0.4}$
GW190929_012149	$104.3^{+34.9}_{-25.2}$	$35.8^{+14.9}_{-8.2}$	$80.8^{+33.0}_{-33.2}$	$24.1^{+19.3}_{-10.6}$	$0.01^{+0.34}_{-0.33}$	$2.13^{+3.65}_{-1.05}$	$0.38^{+0.49}_{-0.17}$	$101.5^{+33.6}_{-25.3}$	$0.66^{+0.20}_{-0.31}$	2200	$10.1^{+0.6}_{-0.8}$
GW190930_133541	$20.3^{+8.9}_{-1.5}$	$8.5^{+0.5}_{-0.5}$	$12.3^{+12.4}_{-2.3}$	$7.8^{+1.7}_{-3.3}$	$0.14^{+0.31}_{-0.15}$	$0.76^{+0.36}_{-0.32}$	$0.15^{+0.06}_{-0.06}$	$19.4^{+9.2}_{-1.5}$	$0.72^{+0.07}_{-0.06}$	1700	$9.5^{+0.3}_{-0.5}$

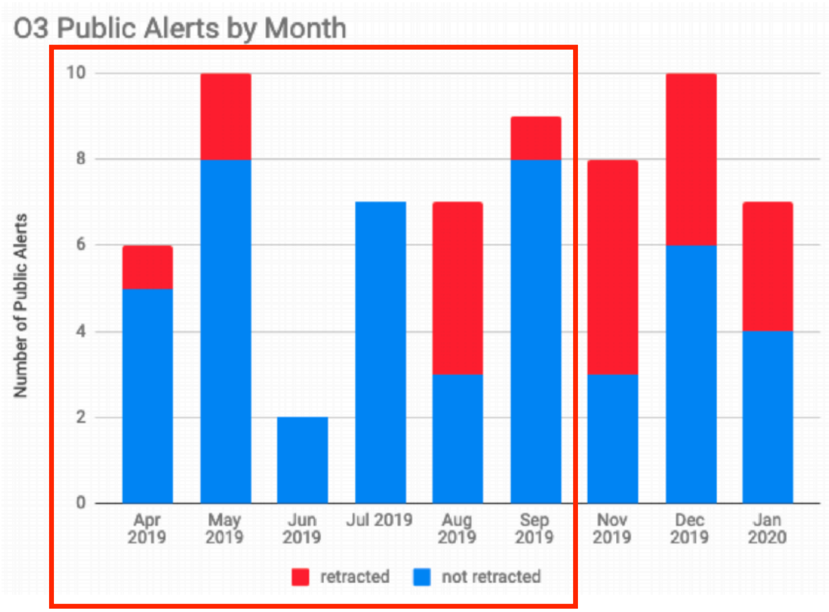

O3a (Apr – Sep 2019)
39 events, 3 with $M < 3\ M_{SUN}$:

GW 190425 -> BNS, 10^4 deg^2 skymap
GW 190426 -> BHNS, 10^3 deg^2 skymap
GW190814 -> (?) BHNS, 19 deg^2 skymap

Waiting for the release of the O3b catalog

GW 190814

The Astrophysical Journal Letters, 896:L44 (20pp), 2020 June 20 https://doi.org/10.3847/2041-8213/ab960f

CrossMark

GW190814: Gravitational Waves from the Coalescence of a 23 Solar Mass Black Hole with a 2.6 Solar Mass Compact Object

R. Abbott[1], T. D. Abbott[2], S. Abraham[3], F. Acernese[4,5], K. Ackley[6], C. Adams[7], R. X. Adhikari[1], V. B. Adya[8], C. Affeldt[9,10], M. Agathos[11,12], K. Agatsuma[13], N. Aggarwal[14], O. D. Aguiar[15], A. Aich[16], L. Aiello[17,18], A. Ain[3], P. Ajith[19], S. Akcay[11,20],

Abstract

We report the observation of a compact binary coalescence involving a 22.2–24.3 $M_\odot$ black hole and a compact object with a mass of 2.50–2.67 $M_\odot$ (all measurements quoted at the 90% credible level). The gravitational-wave signal, GW190814, was observed during LIGO's and Virgo's third observing run on 2019 August 14 at 21:10:39 UTC and has a signal-to-noise ratio of 25 in the three-detector network. The source was localized to 18.5 deg^2 at a distance of 241^{+41}_{-45} Mpc; no electromagnetic counterpart has been confirmed to date. The source has the most unequal mass ratio yet measured with gravitational waves, $0.112^{+0.008}_{-0.009}$, and its secondary component is either the lightest black hole or the heaviest neutron star ever discovered in a double compact-object system. The dimensionless spin of the primary black hole is tightly constrained to $\leqslant 0.07$. Tests of general relativity reveal no measurable deviations from the theory, and its prediction of higher-multipole emission is confirmed at high confidence. We estimate a merger rate density of 1–23 Gpc^{-3} yr^{-1} for the new class of binary coalescence sources that GW190814 represents. Astrophysical models predict that binaries with mass ratios similar to this event can form through several channels, but are unlikely to have formed in globular clusters. However, the combination of mass ratio, component masses, and the inferred merger rate for this event challenges all current models of the formation and mass distribution of compact-object binaries.

GW 190814

21:10:39 UT

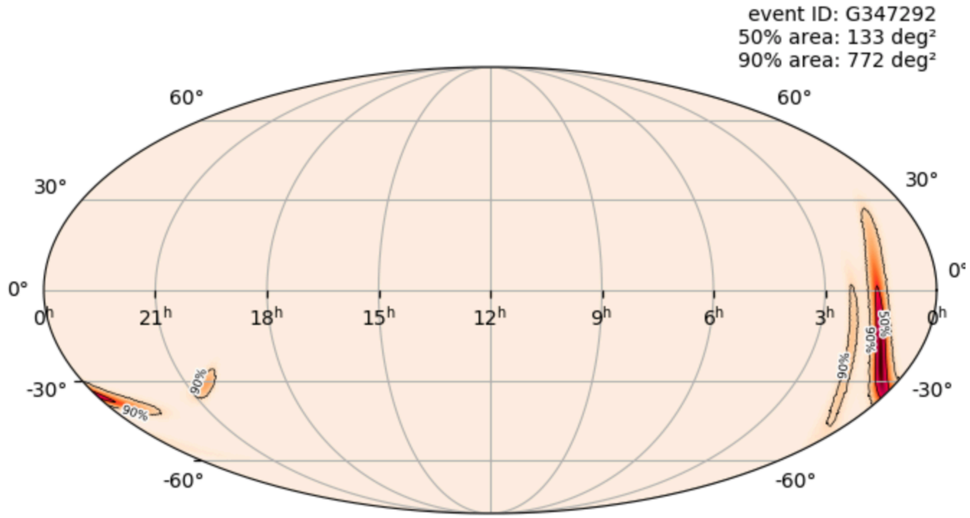

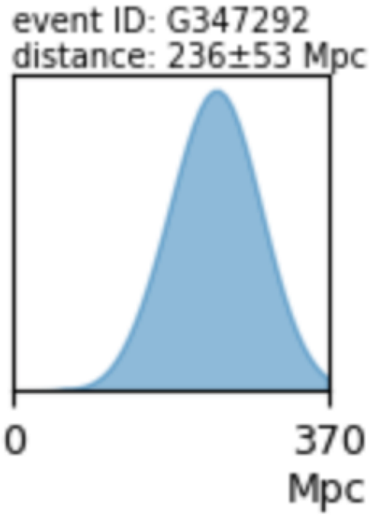

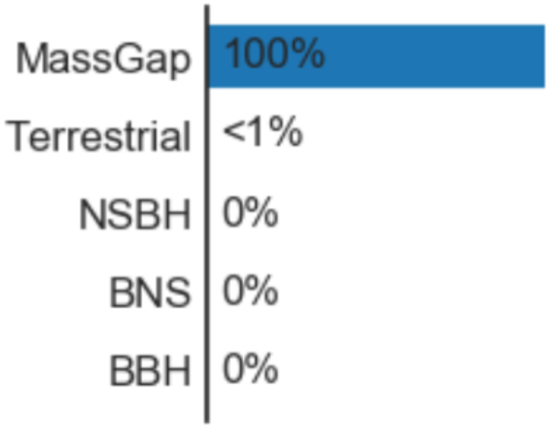

GW 190814

21:10:39 UT

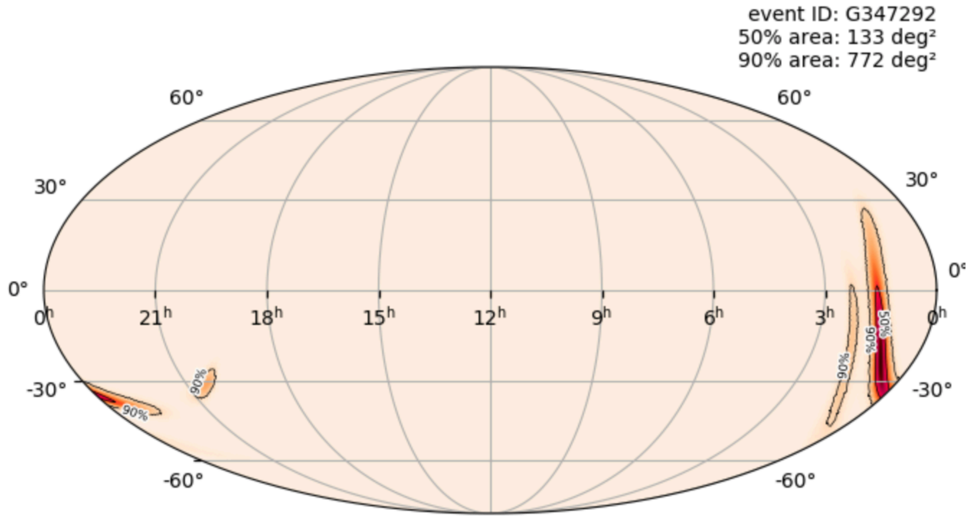

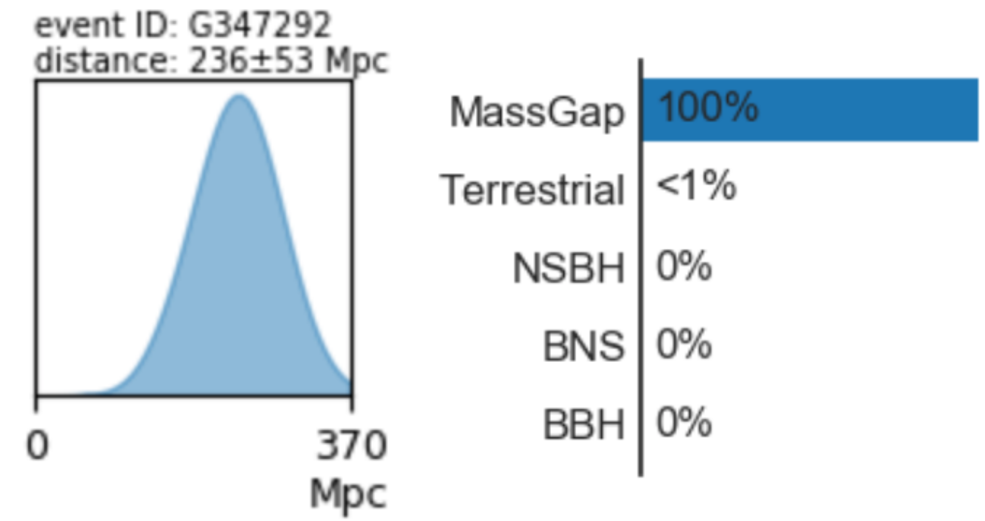

+11.6 h

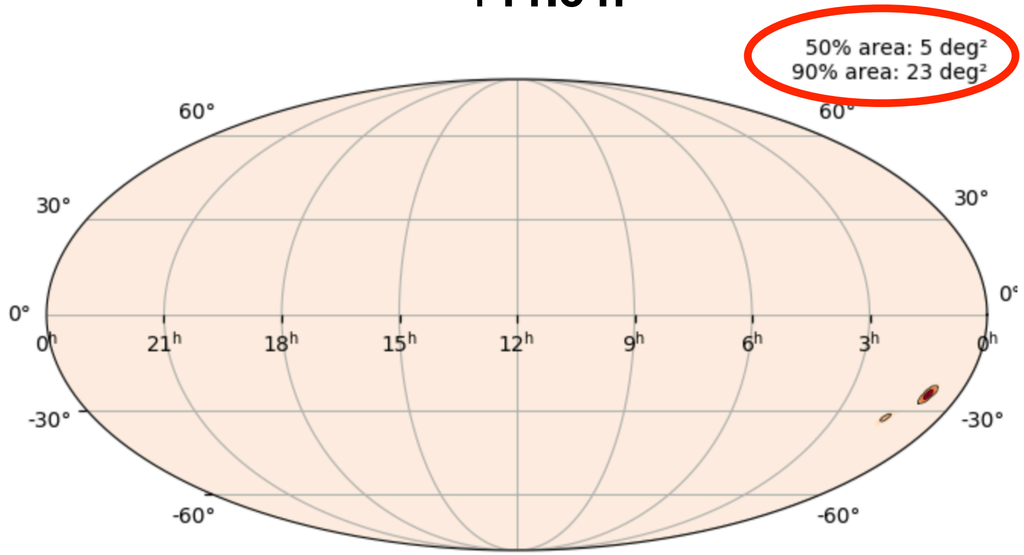

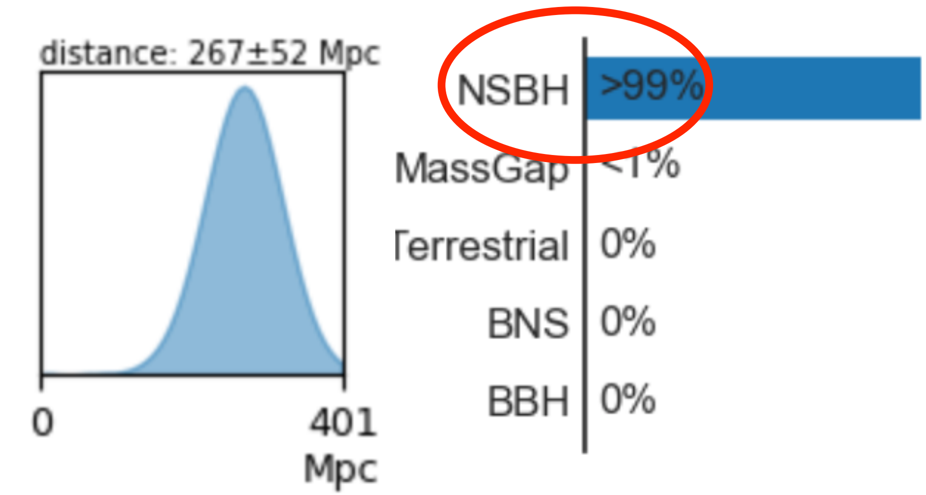

GW 190814: e.m. follow up

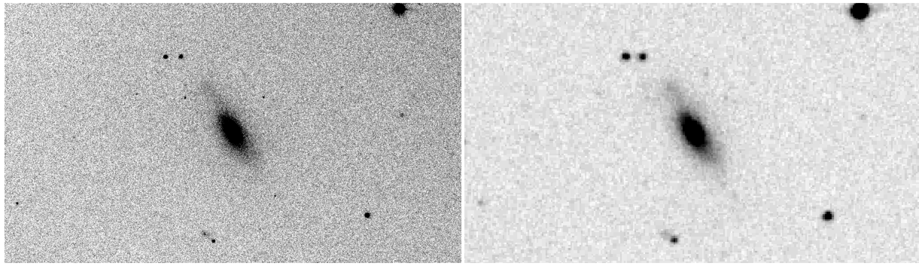

GTC, VLT, LBT, WHT, TNG, NOT, LT, GROND coordinated observations of more than 70 galaxies, over multiple epochs within the 90% localization of the GW

+

Wide-field observations (VST, PS, ATLAS, GOTO)

No e.m. counterpart found

Ackley+20 (ENGRAVE collaboration)

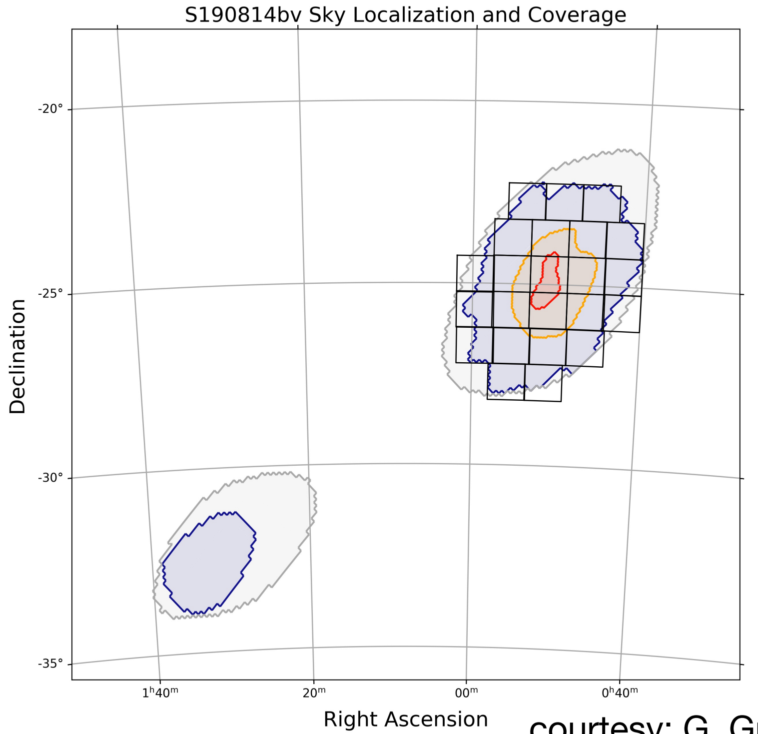

courtesy: G. Greco

5 VST epochs

Δt	r AB mag	Probability
+11.5 h	20.9	60.7%
+1.5 d	21.9	71.5%
+4.3 d	21.7	87.7%
+7.2 d	21.8	87.7%
+14.5 d	22.0	87.7%

Some numbers

- During **O1** (Sep 2015 – Jan 2016) and **O2** (Nov 2016 - Aug 2017) we carried out observational campaigns aimed at the search of e.m. counterparts and follow-up of promising e.m. candidate counterparts of **7 GW triggers (including the successful GW 170817 campaign)**.

Some numbers

- During **O1** (Sep 2015 – Jan 2016) and **O2** (Nov 2016 - Aug 2017) we carried out observational campaigns aimed at the search of e.m. counterparts and follow-up of promising e.m. candidate counterparts of **7 GW triggers (including the successful GW 170817 campaign)**.

- During **O3** (Apr 2019 – Mar 2020) we carried out observational campaigns aimed at the search of e.m. counterparts and follow-up of promising e.m. candidate counterparts of **13 GW triggers**.

- **After the end of O3** (due to the COVID pandemic) we focused our observational activities on the follow-up of KNe candidates found in surveys and of well-localised (< 50 deg2) short GRBs found by Fermi/GBM. On this topic, we observed **2 KN candidates,1 short GRB,**
1 candidate off-axis afterglow of a short GRB.

Some numbers

- During O1 (Sep 2015 – Jan 2016) and O2 (Nov 2016 - Aug 2017) we carried out observational campaigns aimed at the search of e.m. counterparts and follow-up of promising e.m. candidate counterparts of 7 GW triggers.

-During O3 (Apr 2019 – Mar 2020) we carried out observational campaigns aimed at the search of e.m. counterparts and follow-up of promising e.m. candidate counterparts of 13 GW triggers.

-After the end of O3 (due to the COVID pandemic) we focused our observational activities on the follow-up of KNe candidates found in surveys and of well-localised (< 50 deg2) short GRBs found by Fermi/GBM. On this topic, we observed 2 KN candidates,1 short GRB, 1 candidate off-axis afterglow of a short GRB.

Since 2015 we published:
- 64 GCN Circulars, ATel, Astronote
- 8 refereed papers (546 cit., 68 cit./paper) -> GRAWITA-led
- 3 refereed paper (2132 cit., 711 cit./paper) -> GRAWITA participation
- 32 refereed paper (2258 cit, 71 cit./paper) -> GW/KN related papers with participation of (or led by) GRAWITA scientists
- of the above, 9 circulars and 6 papers are based on TNG data (274 cit., 46 cit./paper)

Some numbers

- During O1 (Sep 2015 – Jan 2016) and O2 (Nov 2016 - Aug 2017) we carried out observational campaigns aimed at the search of e.m. counterparts and follow-up of promising e.m. candidate counterparts of 7 GW triggers.

-During O3 (Apr 2019 – Mar 2020) we carried out observational campaigns aimed at the search of e.m. counterparts and follow-up of promising e.m. candidate counterparts of 13 GW triggers.

-After the end of O3 (due to the COVID pandemic) we focused our observational activities on the follow-up of KNe candidates found in surveys and of well-localised (< 50 deg2) short GRBs found by Fermi/GBM. On this topic, we observed 2 KN candidates,1 short GRB, 1 candidate off-axis afterglow of a short GRB.

Since 2015 we published:
- 64 GCN Circulars, ATel, Astronote
- 8 refereed papers (546 cit., 68 cit./paper) -> GRAWITA-led
- 3 refereed paper (2132 cit., 711 cit./paper) -> GRAWITA participation
- 32 refereed paper (2258 cit, 71 cit./paper) -> GW/KN related papers with participation of (or led by) GRAWITA scientists
- of the above, 9 circulars and 6 papers are based on TNG data (274 cit., 46 cit./paper)

- We have been awarded of 435 hours of observing time at TNG over 15 semesters (29 h/semester on average). Current LTP will run up to Feb 2023.

Waiting for O4 (> Jun 2022)

		Area (deg^2) 90% c.r.	Area (deg^2) 90% c.r.	Area (deg^2) 90% c.r.
O3	HLV	270^{+34}_{-20}	330^{+24}_{-31}	280^{+30}_{-23}
→ O4	HLVK	33^{+5}_{-5}	50^{+8}_{-8}	41^{+7}_{-6}

		Comoving Volume (10^3 Mpc^3) 90% c.r.	Comoving Volume (10^3 Mpc^3) 90% c.r.	Comoving Volume (10^3 Mpc^3) 90% c.r.
O3	HLV	120^{+19}_{-24}	860^{+150}_{-150}	16000^{+2200}_{-2500}
→ O4	HLVK	52^{+10}_{-9}	430^{+100}_{-78}	7700^{+1500}_{-920}

Observation Run	Network	Expected BNS Detections	Expected NSBH Detections	Expected BBH Detections
O3	HLV	1^{+12}_{-1}	0^{+19}_{-0}	17^{+22}_{-11}
→ O4	HLVK	10^{+52}_{-10}	1^{+91}_{-1}	79^{+89}_{-44}

Abbott+20 (LRR)

Conclusions & Future

We are at the dawn of a new, exciting, promising, era for astrophysics. No doubt that there is a lot of attention, efforts, planning, expectations from the international community.

Basically all the main forthcoming facilities have multi-messenger astrophysics in their science case (or will play anyway a role): VRO (LSST), CTA, SKA, JWST, e-ELT.
We (GRAWITA and INAF more in general) are involved in all of them.

The TNG characteristics and the diversity of its instrumentation represent a key asset in this context. Working in collaborations and consortia having access to different facilities (all sizes, all wavelengths) ensure an optimal use of the telescope.

Great collaboration and interaction with TNG Director and Staff
(davvero, grazie ragazzi!)

GW 190814: e.m. follow up

Gomez+19

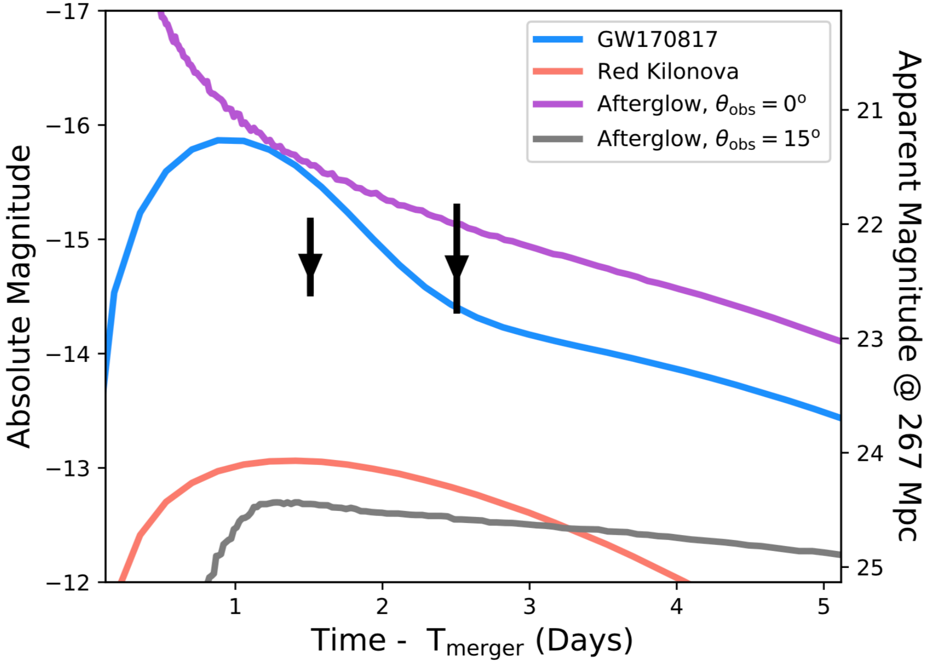

Andreoni+19

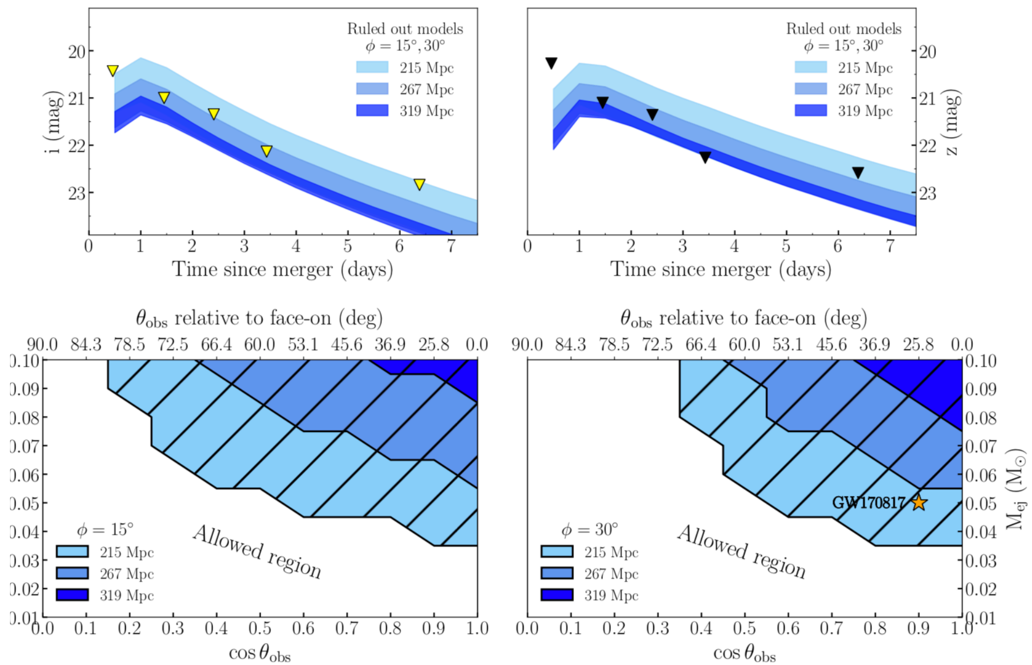

Strong constraints if the lower distance of S190814bv is assumed